



Search for $W' \rightarrow t\bar{b}$ decays in the hadronic final state using pp collisions at $\sqrt{s} = 13$ TeV with the ATLAS detector

The ATLAS Collaboration*



ARTICLE INFO

Article history:

Received 25 January 2018

Received in revised form 13 March 2018

Accepted 13 March 2018

Available online 4 April 2018

Editor: W.-D. Schlatter

ABSTRACT

A search for W' -boson production in the $W' \rightarrow t\bar{b} \rightarrow q\bar{q}'b\bar{b}$ decay channel is presented using 36.1 fb⁻¹ of 13 TeV proton–proton collision data collected by the ATLAS detector at the Large Hadron Collider in 2015 and 2016. The search is interpreted in terms of both a left-handed and a right-handed chiral W' boson within the mass range 1–5 TeV. Identification of the hadronically decaying top quark is performed using jet substructure tagging techniques based on a shower deconstruction algorithm. No significant deviation from the Standard Model prediction is observed and the results are expressed as upper limits on the $W' \rightarrow t\bar{b}$ production cross-section times branching ratio as a function of the W' -boson mass. These limits exclude W' bosons with right-handed couplings with masses below 3.0 TeV and W' bosons with left-handed couplings with masses below 2.9 TeV, at the 95% confidence level.

© 2018 The Author. Published by Elsevier B.V. This is an open access article under the CC BY license (<http://creativecommons.org/licenses/by/4.0/>). Funded by SCOAP³.

1. Introduction

Several theories beyond the Standard Model (SM) involve enhanced symmetries that predict new gauge bosons, usually called W' or Z' bosons. The W' boson is the mediator of a new charged vector current that can be massive enough to decay into a top quark and a b -quark (as in Fig. 1). Many models such as those with extra dimensions [1], strong dynamics [2–5], composite Higgs [6], or the Little Higgs [7,8] predict new vector charged-current interactions, some with preferential couplings to quarks or third-generation particles [6,9–12]. Due to the large mass of the top quark, its interactions decouple from the rest of the phenomenology in many theories beyond the SM. An effective Lagrangian is used to capture the relevant phenomenology of the Sequential Standard Model (SSM) [13] $W' \rightarrow t\bar{b}$ signal [14,15], which has the same coupling strength to fermions as the SM W boson but higher mass.

Searches for a W' boson decaying into $t\bar{b}$,¹ classified as either leptonic or hadronic according to the decay products of the W boson originating from the top quark, were performed at the Tevatron [16,17] and the Large Hadron Collider (LHC) in final states that include leptons [18–21] or that are fully hadronic [22]. The specific search for a W' boson decaying into $t\bar{b}$ allows for a right-handed W' boson (W'_R) in models in which the right-handed neutrino's mass is assumed to be much higher than that of the W' boson

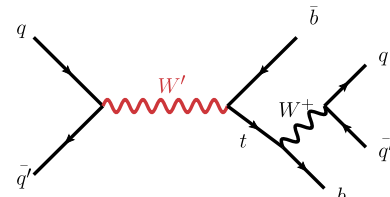


Fig. 1. Feynman diagram for W' -boson production with decay into $t\bar{b}$ and a hadronically decaying top quark.

($m_{\nu_R} > m_{W'}$), which the leptonic decay mode cannot access. In such a model, the branching ratio for a W'_R boson decaying into $t\bar{b}$ is $\mathcal{O}(10\%)$ higher relative to that for a W'_L boson decaying into $t\bar{b}$ since a W'_L boson can also decay to a lepton and neutrino. Limits on a SSM left-handed W' boson (W'_L) decaying into a lepton and a neutrino have been set previously [23,24]. Previous searches in the all-hadronic final state exclude W'_R bosons with masses up to 2 TeV, set at the 95% confidence level (CL) using 20.3 fb⁻¹ of pp collision data at a centre-of-mass energy (\sqrt{s}) of 8 TeV [22]. A recent search by the CMS Collaboration in the lepton+jets final state excludes W'_R -boson masses up to 3.6 TeV using 35.9 fb⁻¹ of pp collision data collected at $\sqrt{s} = 13$ TeV [18].

This analysis searches for a W' boson decaying into $t\bar{b}$ with a mass in the range of 1–5 TeV, in the invariant mass spectrum of the top quark and bottom quark ($m_{t\bar{b}}$) reconstructed in the fully hadronic channel. This includes a W'_R boson that is not kinematically allowed to decay into a lepton and neutrino and a W'_L boson that can decay into quarks or leptons. The large W' mass results

* E-mail address: atlas.publications@cern.ch.

¹ For simplicity, the notation “ $t\bar{b}$ ” is used to denote the final state for both $W'^+ \rightarrow t\bar{b}$ and $W'^- \rightarrow \bar{t}b$ decays.

in a top quark and a b -quark that have high transverse momentum (p_T).² The decay products of the top quark become more collimated as the top-quark p_T increases, and their showers partially overlap [25]. This high- p_T topology is referred to as *boosted*. The boosted top-quark decay is reconstructed as a single jet. The shower deconstruction (SD) algorithm [26,27] is employed to select, or tag, jets from boosted top-quark decays. A signal would be reconstructed as a localised excess in the m_{tb} distribution rising above the smoothly falling background originating mostly from jets created by the strong interaction described by quantum chromodynamics (QCD). This analysis represents an improvement on the previous ATLAS analysis in this channel [22] due to a higher centre-of-mass energy, higher integrated luminosity, and better top-tagging techniques, understanding of systematic uncertainties, and statistical treatment.

2. ATLAS detector

The ATLAS detector [28] at the LHC covers almost the entire solid angle around the collision point. Charged particles in the pseudorapidity range $|\eta| < 2.5$ are reconstructed with the inner detector (ID), which consists of several layers of semiconductor detectors (pixel and strip) and a straw-tube transition-radiation tracker, the latter covering $|\eta| < 2.0$. The high-granularity silicon pixel detector provides four measurements per track; the closest layer to the interaction point is known as the insertable B-layer (IBL) [29]. The IBL was added in 2014 and provides high-resolution hits at small radius to improve the tracking performance. The ID is immersed in a 2 T magnetic field provided by a superconducting solenoid. The solenoid is surrounded by electromagnetic and hadronic calorimeters, and a muon spectrometer incorporating three large superconducting toroid magnet systems. The calorimeter system covers the pseudorapidity range $|\eta| < 4.9$. Electromagnetic calorimetry is performed with barrel and endcap high-granularity lead/liquid-argon (LAR) electromagnetic calorimeters, within the region $|\eta| < 3.2$. There is an additional thin LAR presampler covering $|\eta| < 1.8$, to correct for energy loss in material upstream of the calorimeters. For $|\eta| < 2.5$, the LAR calorimeters are divided into three layers in depth. Hadronic calorimetry is performed with a steel/scintillator-tile calorimeter, segmented into three barrel structures within $|\eta| < 1.7$, and two copper/LAR hadronic endcap calorimeters, which cover the region $1.5 < |\eta| < 3.2$. The forward solid angle up to $|\eta| = 4.9$ is covered by copper/LAR and tungsten/LAR calorimeter modules, which are optimised for energy measurements of electrons/photons and hadrons, respectively. The muon spectrometer (MS) comprises separate trigger and high-precision tracking chambers that measure the deflection of muons in a magnetic field generated by superconducting air-core toroids. The ATLAS detector uses a tiered trigger system to select interesting events. The first level is implemented in custom electronics and reduces the event rate from the LHC crossing frequency of 40 MHz to a design value of 100 kHz. The second level is implemented in software running on a general-purpose processor farm which processes the events and reduces the rate of recorded events to ~ 1 kHz [30].

² ATLAS uses a right-handed coordinate system with its origin at the nominal interaction point (IP) in the centre of the detector and the z -axis along the beam pipe. The x -axis points from the IP to the centre of the LHC ring, and the y -axis points upwards. Cylindrical coordinates (r, ϕ) are used in the transverse plane, ϕ being the azimuthal angle around the z -axis. The pseudorapidity is defined in terms of the polar angle θ as $\eta = -\ln \tan(\theta/2)$. Angular separation is measured in units of $\Delta R \equiv \sqrt{(\Delta\eta)^2 + (\Delta\phi)^2}$, where $\Delta\eta$ and $\Delta\phi$ are the separations in η and ϕ . Momentum in the transverse plane is denoted by p_T .

3. Data and simulation samples

This analysis uses data from proton–proton (pp) collisions at $\sqrt{s} = 13$ TeV collected with the ATLAS detector in 2015 and 2016 that satisfy a number of criteria to ensure that the ATLAS detector was in good operating condition. The amount of data used in this analysis corresponds to an integrated luminosity of 36.1 fb^{-1} . The average number of pp interactions delivered per LHC bunch crossing was 23.7.

Monte Carlo (MC) event generators were used to simulate signal and background events. Signal events were generated at leading order (LO) in QCD by MADGRAPH5_AMC@NLO v2.2.3 [31], using a chiral W' -boson model in which the coupling strength of the W' boson to the right- and left-handed fermions are the same as those of the SM W boson to left-handed fermions. The W'_L boson can decay into all left-handed fermions, but the W'_R boson can decay only into right-handed quarks as the right-handed neutrino is assumed to be more massive than the W'_R boson. MADGRAPH was used to simulate the top-quark and W -boson decays, taking spin correlations into account. PYTHIA v8.186 [32] was used for the modelling of the parton shower, fragmentation and the underlying event. The NNPDF23LO parton distributions function (PDF) set [33] and the A14 set of tuned parameters [34] were used for the event generation. All simulated samples were rescaled to next-to-leading-order (NLO) calculations using NLO/LO K -factors ranging from 1.3 to 1.4, depending on the mass and handedness of the W' boson, calculated with ZTOP [15]. The width of the MADGRAPH simulated W' boson is set to the NLO ZTOP width calculation, $\mathcal{O}(3\%)$ of its mass. Signal samples with gauge-boson masses between 1 and 3 TeV were generated in 250 GeV steps, and between 3 and 5 TeV in 500 GeV steps.

The dominant SM background process is multi-jet production. In order to reduce the dependence on the modelling of the simulation a data-driven method is implemented as described in Section 5. Corrections in this method are estimated using QCD dijet simulation produced at LO by PYTHIA v8.186. Uncertainties in this method are obtained using simulated QCD dijet events produced at LO by HERWIG++ v2.7.1 [35] and SHERPA v2.1.1 [36], and at NLO by POWHEG-Box v2 [37,38] with either PYTHIA8 or HERWIG+JIMMY [39] for the parton shower, fragmentation and the underlying event simulation (referred to as POWHEG+PYTHIA and POWHEG+HERWIG, respectively). Vector bosons (W/Z) produced in association with jets are included in the data-driven approach. These processes are expected to contribute less than 1% of the multi-jet background. This W/Z +jets prediction is checked using events simulated with the SHERPA v2.2.1 [36] generator and the CT10 PDF set [40].

Top-quark pair production is an important background with an inclusive cross-section of $\sigma_{t\bar{t}} = 832^{+46}_{-51} \text{ pb}$ for a top-quark mass of 172.5 GeV as obtained from calculations accurate to next-to-next-to-leading order and next-to-next-to-leading logarithms (NNLO+NNLL) in QCD with Top++2.0 [41–47]. Simulated top-quark pair processes were produced using the NLO POWHEG-Box v2 generator with the CT10 PDF. The parton shower, fragmentation and the underlying event were added using PYTHIA v6.42 [48] with the Perugia 2012 set of tuned parameters [49]. To increase the number of simulated events at high mass, samples were produced binned in $t\bar{t}$ mass. Interference and background contributions from the SM s -channel single-top process are found to be negligible and are not considered further in this analysis.

The generation of the simulated event samples includes the effect of multiple pp interactions per bunch crossing, as well as the effect on the detector response due to interactions from bunch crossings before or after the one containing the hard interaction. For all MADGRAPH, POWHEG, PYTHIA and HERWIG samples, the EvtGen v1.2.0 program [50] was used for the bottom and charm

hadron decays. The simulated samples were passed through the GEANT4-based ATLAS detector simulation [51,52] and were reconstructed with the same algorithms as the data events.

4. Event reconstruction and shower deconstruction

4.1. Event reconstruction

This analysis relies on the reconstruction and identification of jets initiated by the top- and bottom-quark daughters of the W' boson. Jets are built from topologically related energy depositions in the calorimeters with the anti- k_t algorithm [53] using the FastJet package [54]. Two radius parameters are used for jet reconstruction: a small radius (small- R) of 0.4 and a large radius (large- R) of 1.0. The momenta of both the small- R and large- R jets are corrected for energy losses in passive material and for the non-compensating response of the calorimeter [55]. Small- R jets are also corrected for the average additional energy due to pile-up interactions [56]. Energy depositions from pile-up are removed from large- R jets using the trimming algorithm [57]: the constituents of the large- R jet are reclustered using the k_t jet algorithm [58, 59] with $R = 0.2$. Constituent jets contributing less than 5% of the large- R jet's p_T are removed. The remaining energy depositions are used to calculate the trimmed-jet kinematics and substructure properties. In order to improve on the angular resolution of the calorimeter, the mass of a large- R jet is computed using a combination of calorimeter and tracking information [60].

Small- R jets are used to identify the jets compatible with originating from a b -quark created either directly from the W' boson or from the top-quark decay. Only small- R jets with $p_T > 25$ GeV and $|\eta| < 2.5$ (in order to be within the coverage of the ID) are considered in this analysis. Additional p_T requirements are applied to enhance the sensitivity of the search (see Section 5). To reduce the number of small- R jets originating from pile-up interactions, a likelihood discriminant, based on track and vertex information, is used to determine whether the primary vertex³ is the origin of the charged-particle tracks associated with a jet candidate and rejects jets originating from pile-up interactions [61]. This is done only for small- R jets with $p_T < 60$ GeV and $|\eta| < 2.4$. Small- R jets which originate from b -quarks are identified using a multivariate b -tagging algorithm [62,63]. Several observables, such as those based on the long lifetime of b -hadrons and the b - to c -hadron decay topology, are used as algorithm inputs to discriminate between b -jets, c -jets and other jets. The b -tagging requirement corresponding to an efficiency of 77% to identify b -jets with $p_T > 20$ GeV, as determined from a sample of simulated $t\bar{t}$ events, is found to be optimal for the statistical significance of this search. This 77% working point (WP) provides rejection factors against light-flavour/gluon jets and c -jets of 134 and 6 respectively [63,64]. Jets identified this way are referred to as b -tagged jets. Since the b -tagging factors are measured in a different p_T region, an uncertainty is assigned to the extrapolation of the measurement to the high p_T region of interest.

Events with reconstructed electrons [65] or muons [66] are vetoed in order to ensure statistical independence of this analysis from analyses using the leptonic decay of the W boson from the top quark [19]. Electrons and muons with transverse momenta above 25 GeV and selected with criteria similar to those used in Ref. [67] are considered for this veto.

³ Collision vertices are formed from tracks with $p_T > 400$ MeV. If an event contains more than one vertex candidate, the one with the highest $\sum p_T^2$ of its associated tracks is selected as the primary vertex.

4.2. Boosted-top identification using shower deconstruction

The SD algorithm can be used to identify the jets compatible with the hadronic decay of a W/Z boson, Higgs boson, or a top quark as well as to discriminate between quark- and gluon-initiated jets. In this analysis, an SD-algorithm-based tagger (SD tagger) is used to identify jets originating from the top quark. The SD tagger calculates likelihoods that a given large- R jet originates from a hadronic top-quark decay or from a high-momentum light quark or gluon. The constituents of the trimmed large- R jet are used to build exclusive subjets [54], and the four-momenta of these subjets serve as inputs to the SD algorithm. These subjets are used as substitutes for individual quarks and gluons originating from the hard scatter. A likelihood weight is calculated for each possible shower history that can lead to the observed subjet configuration. This step is analogous to running a parton shower MC generator in reverse, where emission and decay probabilities at each vertex, colour connections, and kinematic requirements are considered. For each shower history, the assigned weight is proportional to the probability that the assumed initial particle generates the final configuration, taking into account the SM amplitude for the underlying hard process and the Sudakov form factors for the parton shower. A variable called χ_{SD} is defined as the ratio of the sum of the signal-hypothesis weights to the sum of the background-hypothesis weights. For a set $\{p_i^k\}$ of N observed subjet four-momenta, where $i \in [1, N]$, the value of χ_{SD} is given by:

$$\chi_{SD}(\{p_i^k\}) = \frac{\sum_{\text{perm}} P(\{p_i^k\}|\text{top-quark jet})}{\sum_{\text{perm}} P(\{p_i^k\}|\text{gluon/light-quark jet})},$$

where $P(\{p_i^k\}|\text{top-quark jet})$ is built using the weights for the hypothesis that a signal process leads to the observed subjet configuration $\{p_i^k\}$ and $P(\{p_i^k\}|\text{gluon/light-quark jet})$ is built using the weights for the hypothesis that a background process leads to the observed subjet configuration. The \sum_{perm} notation represents the sum over all the shower histories in which signal processes lead to the subjet configuration. The large- R jet is tagged as a top-quark jet if χ_{SD} is larger than a given value, which is adjusted to achieve the desired tagging efficiency. There is an internal mechanism in the SD algorithm to suppress pile-up contributions to the jets, through the application of additional weights in the likelihood ratio, which contain the probability that a subset of the subjets did not originate from the hard interaction but from pile-up [68].

The SD algorithm selects events that are kinematically compatible with a hadronic top-quark decay. The following requirements are made to optimise the algorithm to achieve a balance between good top-quark jet signal selection efficiency and rejection of gluon/light-quark jet backgrounds: the large- R jet has at least three subjets; two or more subjets must have a combined invariant mass in a 60.3–100.3 GeV window centred on the W -boson mass; and at least one more subjet can be added to obtain a total mass in a 132–212 GeV window centred on the top-quark mass.

The SD tagger was optimised for this analysis so that it is more efficient for top-quark jet signal selection and gluon/light-quark jet background rejection for $p_T > 800$ GeV compared to the version of the SD tagger first studied by the ATLAS Collaboration [25]. This is done by building subjets obtained by using an exclusive k_t algorithm [54]. First, the k_t algorithm with $R = 1.0$ is run over the large- R jet constituents and the k_t reclustering is stopped if the splitting scale [69] is larger than 15 GeV. Once the k_t reclustering is stopped the reclustered protojets are used as subjets. The choice of a 15 GeV requirement is based on the expected discrimination between signal and background events. The six highest p_T

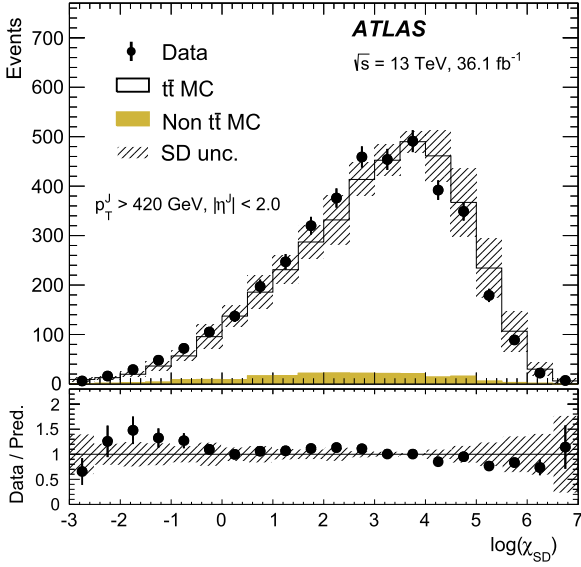


Fig. 2. Comparison of the $\log(\chi_{SD})$ distribution between data (dots), $t\bar{t}$ MC events (line histogram) and background MC events (solid histogram) in samples with an enriched contribution from hadronically decaying top quarks using selection criteria similar to those in Ref. [25]. The hatched band shows the effect of the SD uncertainty described in Section 6.

subjects are used as inputs to the SD algorithm. This reduces the computation time needed for the calculation of χ_{SD} , which grows exponentially with the subject multiplicity, without loss of background rejection power.

The signal efficiency WP of the SD tagger is set by applying a selection on the logarithm of χ_{SD} . The 50% and 80% signal efficiency WPs are used in this analysis (see Section 5). The background rejection for the 50% (80%) signal efficiency WP is 80 (25) for a jet p_T of 0.45 TeV and 30 (10) for a p_T of 1.3 TeV. The $\log(\chi_{SD})$ variable is studied using samples enriched in hadronically decaying top quarks by selecting $t\bar{t}$ events where one top quark decays hadronically and the other into lepton+jets for events with large- R jet p_T (p_T^j) $>$ 420 GeV and $|\eta|$ ($|\eta^j|$) $<$ 2.0. To obtain a top-quark-enriched sample, events are selected with two b -tagged jets and either an electron or muon using criteria similar to those used in Ref. [25]. The data are found to be consistent with simulation in the $\log(\chi_{SD})$ distribution within the SD tagger uncertainty, described in Section 6, as shown in Fig. 2.

5. Event selection and background estimation

An initial selection of events is made at the trigger level by requiring at least one small- R jet [30] with p_T larger than 380 GeV.

To ensure that the analysis is performed in the fully efficient regime of the trigger, the p_T values of the large- R and small- R jets, used to identify the top- and b -quark daughters from the W' -boson decay, are required to be larger than 420 GeV. Candidate events must have at least one primary vertex.

The top-quark jet candidate is selected from the large- R jets satisfying the requirements defined in Section 4. The large- R jet with the largest value of $m_j + 0.15 \times m_j$, where m_j is the mass of the highest- p_T small- R jet with minimum $p_T > 25$ GeV with $\Delta R < 1.0$ of the large- R jet and m_j is the mass of the large- R jet, is selected as the top-quark jet candidate. This combination enhances the fraction of events where the selected large- R jet is associated with the top quark, since m_j is less affected by final-state radiation effects, which are important at high p_T [70]. The highest- p_T small- R jet with $p_T > 420$ GeV and $\Delta R > 2.0$ from the top-quark jet candidate is chosen as the b -quark jet candidate in the event. The top- and b -tagging criteria are applied to the selected top- and b -quark jet candidates after rejecting events in which the b -quark jet candidate has $|\eta| > 1.2$. This improves the signal sensitivity at high m_{tb} since the high- p_T b -quark jets from the W' -boson decay tend to be more central (smaller $|\eta|$) than the jets from the multi-jet background. A summary of the top- and b -quark jet candidate selection is shown in Table 1.

Events are divided into two categories: the “1 b -tag in” category and the “0 b -tag in” category. For the “1 b -tag in” category, exactly one b -tagged small- R jet with $p_T > 25$ GeV with $\Delta R < 1.0$ from the top-quark jet candidate is required, while for the “0 b -tag in” category, it is required that there be zero b -tagged small- R jets with $p_T > 25$ GeV within the large- R jet.

The binning of the m_{tb} distribution is chosen to balance the sensitivity coming from the different signal and background distribution shapes against the diminishing statistical sensitivity of the data at high m_{tb} . Requirements are imposed on the expected number of background events per bin and the bin width is adapted to a resolution function that represents the width of the reconstructed mass peak for each studied W' -boson signal sample. For each m_{tb} bin and in each of the “ b -tag in” categories, the data sample is divided into six regions by using top-tagging and b -tagging criteria, which are described in Fig. 3. The “not loose top-tagged” regions consist of events where the selected top-quark jet candidate fails to meet the loose top-tagged (80% WP) identification criteria, the “loose-but-not-tight top-tagged” regions consist of events where the selected top-quark jet candidate satisfies the loose top-tagged identification criteria but not the tight top-tagged criteria (50% WP) and the “tight top-tagged” regions consist of events where the selected top-quark jet candidate satisfies the tight top-tagged criteria. The signal regions are constructed from events in which the selected small- R jet b -candidate is b -tagged: signal region SR1 consists of events classified as “tight top-tagged, 0 b -tag in”, sig-

Table 1

Summary of the top-quark jet candidate and b -quark jet candidate selections before categorisation of events into signal and control regions. The selections are defined in Sections 4 and 5. The events satisfying these criteria are grouped into the categories and regions described in Fig. 3.

Event reconstruction and selection	
Large- R jet (J)	$p_T^j > 420$ GeV, $ \eta < 2.0$
Small- R jet (j)	$p_T^j > 25$ GeV, $ \eta < 2.5$
Top-quark jet candidate (J_{top}^{cand})	jet J with highest $m_j + 0.15 \times m_j$
b -quark jet candidate (J_b^{cand})	highest- p_T jet j with $p_T^j > 420$ GeV, $\Delta R(J_{top}^{cand}, j) > 2.0$
Lepton veto	zero leptons with $p_T > 25$ GeV, $ \eta < 2.5$
b -quark jet candidate η	zero J_b^{cand} with $ \eta > 1.2$
0 b -tag in	zero b -tagged jets j with $\Delta R(J_{top}^{cand}, j) < 1.0$
1 b -tag in	exactly one b -tagged jet j with $\Delta R(J_{top}^{cand}, j) < 1.0$

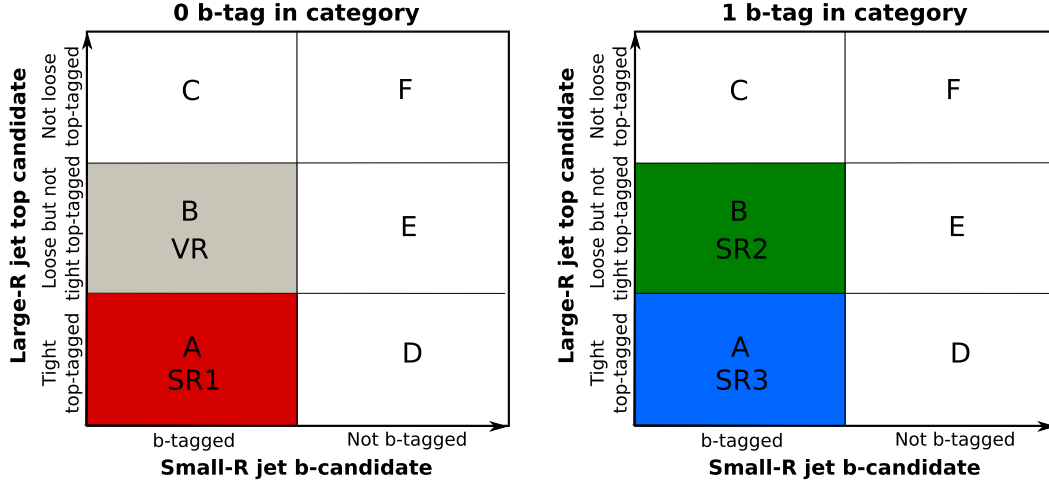


Fig. 3. Illustration of the 2D sideband method showing the two-dimensional plane of the large- R jet substructure variables vs the small- R jet b -tagging information used to estimate the background yield in regions A (B), from the observed yield in the three control regions C, F, D (C, F, E) for the (left) “0 b -tag in” and (right) “1 b -tag in” categories. The top- and b -tagging criteria are applied after rejecting events in which the b -quark jet candidate has $|\eta| > 1.2$.

nal region SR2 consists of events classified as “loose-but-not-tight top-tagged, 1 b -tag in” and signal region SR3 consists of events classified as “tight top-tagged, 1 b -tag in”. A validation region (VR), with negligible signal contamination, is defined to test the performance of the data-driven method of estimating the multi-jet + W/Z +jets background. This region consists of events where the b -candidate is b -tagged, and classified as “loose-but-not-tight top-tagged, 0 b -tag in”. The prediction is found to be in agreement with data within uncertainties.

The W' -boson signal selection efficiency, for masses below 2.5 TeV, is higher in SR2 and SR3 than in SR1, due to the requirement of zero b -tagged jets with $\Delta R < 1.0$ of the large- R jet (“0 b -tag in” category) in SR1, making the topology less like the signal in SR1. For masses above 2.5 TeV, the signal efficiency is higher in SR1 than in SR2 and SR3 for the same reason: the b -tagging efficiency, decreasing with p_T , affects SR2 and SR3 more due to the requirement of the additional b -tagged jet. Thus, the addition of the “0 b -tag in” category improves the signal sensitivity at large W' -boson masses. The W' -boson signal event selection efficiency is about 10% at low mass, decreasing to about 7% at high mass. The difference between the W'_R -boson and W'_L -boson signal selection efficiencies depends on the signal region and the efficiency is on average $\sim 10\%$ higher for W'_R -boson signal samples. The difference in efficiency between W'_R -boson and W'_L -boson signals comes from a difference in angular separation between the W boson and the b -quark from the top-quark decay due to the different W' -boson handedness, leading to a difference in the overall top-tagging efficiency. For instance, the 3 TeV W'_R -boson signal sample has a selection efficiency of 2.9% in SR1, 2.5% in SR2 and 2.4% in SR3, while the 3 TeV W'_L -boson signal sample has a selection efficiency of 2.7% in SR1, 2.3% in SR2 and 2.3% in SR3.

The dominant background from multi-jet production is estimated directly from data using a six-region “2D sideband” method that predicts both the shape and normalisation of the m_{tb} distribution. These regions are shown in Fig. 3.

The amount of multi-jet + W/Z +jets background in the signal regions and in the VR is estimated bin-by-bin in the m_{tb} distribution using the observed number of events in the control regions after subtracting the contribution from $t\bar{t}$ events:

$$N_A^{\text{bkg}} = R_A^{\text{corr}} \cdot \frac{(N_C^{\text{data}} - N_C^{t\bar{t}}) \cdot (N_D^{\text{data}} - N_D^{t\bar{t}})}{N_F^{\text{data}} - N_F^{t\bar{t}}} \text{ and}$$

$$N_B^{\text{bkg}} = R_B^{\text{corr}} \cdot \frac{(N_C^{\text{data}} - N_C^{t\bar{t}}) \cdot (N_E^{\text{data}} - N_E^{t\bar{t}})}{N_F^{\text{data}} - N_F^{t\bar{t}}},$$

where “bkg” stands for multi-jet background and W/Z +jets background, N_A^{bkg} and N_B^{bkg} are the numbers of multi-jet + W/Z +jet background events in regions A and B estimated using this method; N_k^{data} and $N_k^{t\bar{t}}$ ($k = C, D, E, F$) are the numbers of observed events and the expected number of $t\bar{t}$ events in each region, respectively. The correlation between the top- and b -tagging variables (R^{corr}) is evaluated using five simulated QCD dijet samples as:

$$R_A^{\text{corr}} = \frac{N_A^{\text{dijet MC}} \cdot N_F^{\text{dijet MC}}}{N_C^{\text{dijet MC}} \cdot N_D^{\text{dijet MC}}} \text{ and } R_B^{\text{corr}} = \frac{N_B^{\text{dijet MC}} \cdot N_F^{\text{dijet MC}}}{N_C^{\text{dijet MC}} \cdot N_E^{\text{dijet MC}}},$$

where $N^{\text{dijet MC}}$ is the number of events predicted by QCD dijet simulation in a given region. The prediction by PYTHIA is used to correct for this correlation, while the difference between the predictions of the correlation by other QCD dijet simulations (see Section 3) is used to determine the systematic uncertainty of this 2D sideband method. Experimental systematic uncertainties (see Section 6) are found to have a negligible impact on R^{corr} . The value of R^{corr} is found to depend on the signal region and varies between 0.6 at low m_{tb} and 1.3 at high m_{tb} .

The event yields in the different regions considered are shown in Table 2. The multi-jet background makes up more than 90% of the total background in SR1, SR2 and VR, and 75% of the total background in SR3. The contribution of $t\bar{t}$ events is 4%, 9% and 25% of the total background in SR1, SR2 and SR3. The data are well described by the background model. For regions C, D, E and F, the number of multi-jet + W/Z +jets is equal to the number of data events after subtracting the $t\bar{t}$ contribution.

6. Systematic uncertainties

The sources of systematic uncertainty can be broadly divided into three groups: those of experimental nature, those related to the modelling in simulation, and those related to the data-driven multi-jet background estimation.

The simulated samples are affected by uncertainties related to the description of the detector response. The dominant detector-related systematic effects are due to the uncertainties in the jet

Table 2
Event yields in the different regions including the signal regions, SR1, SR2 and SR3. Also shown are the total systematic uncertainties in the estimate of the multi-jet + W/Z +jets and $t\bar{t}$ backgrounds in the different regions. The numbers in parentheses are the percentage fractions of the total background. For regions C, D, E and F, the number of multi-jet + W/Z +jets is equal to the number of data events after subtracting the $t\bar{t}$ contribution.

"0 b-tag in" category						
	SR1	VR	Region C	Region D	Region E	Region F
Data	16,333	57,626	655,669	267,440	958,847	12,591,520
$t\bar{t}$	620 ± 160 (4%)	780 ± 190 (1%)	1,520 ± 310	2,400 ± 600	3,400 ± 900	5,100 ± 1,100
Multi-jet + W/Z +jets	15,200 ± 2,500 (96%)	54,000 ± 12,000 (99%)				
"1 b-tag in" category						
	SR3	SR2	Region C	Region D	Region E	Region F
Data	4,265	12,834	78,326	56,044	187,990	1,224,317
$t\bar{t}$	1,120 ± 290 (25%)	1,140 ± 280 (9%)	1,120 ± 260	5,300 ± 1,200	6,700 ± 1,500	5,600 ± 1,200
Multi-jet + W/Z +jet	3,250 ± 970 (75%)	11,200 ± 2,700 (91%)				

energy scale (JES) and resolution (JER) [71], in the b -tagging efficiency and mistag rate [63] and in the top tagging. The main contributions to the uncertainties in the small- R JES, derived as a function of jet p_T and η , are related to in situ calibration, the dependence on the pile-up activity and on the flavour composition of jets [55,72]. The uncertainty in the scale and resolution of large- R jet energy and mass is evaluated by comparing the ratio of calorimeter-based to track-based measurements in multi-jet data and simulation [25,60]. The flavour-tagging efficiency and its uncertainty for b -jets [62] is estimated in $t\bar{t}$ events, while the misidentification rate for c -jets and other jets and their corresponding uncertainties are determined using a $t\bar{t}$ -enriched region and multi-jet events, respectively. The SD top-tagging uncertainty is estimated by varying the p_T of the subjects used as inputs to the SD algorithm by 2.5%. This value is derived using a procedure described in Ref. [25] and is found to cover any data/simulation differences in the $\log \chi_{SD}$ distribution (see Fig. 2). Systematic uncertainties in the lepton veto are found to have a negligible effect.

Flavour-tagging simulation-to-data efficiency correction factors [62] depend on the jet p_T and η . These correction factors have several sources of uncertainty. They are split into uncorrelated components that are then treated independently. Additional uncertainties are considered in the extrapolation of the b -quark jet and c -jet efficiency calibration from low p_T , where there is enough data to make a measurement, to high p_T .

The average number of interactions per bunch crossing is rescaled in simulation by 9% to improve agreement with data, and an uncertainty, as large as the correction, is assigned. Finally, a global normalisation uncertainty of 2.1% is assigned due to the uncertainty in the luminosity measurement. It is derived, following a methodology similar to that detailed in Ref. [73], from a calibration of the luminosity scale using x-y beam-separation scans performed in August 2015 and May 2016.

The multi-jet background uncertainties pertain primarily to the estimation method itself. Simulation predictions for the correlation between top- and b -tagging criteria in the multi-jet background estimation are one source of uncertainty; different event generators are compared to account for differences in modelling of the matrix element and parton showering. The uncertainty in the total background yield arising from the contribution of multi-jets is 15% in SR1, 22% in SR2 and 22% in SR3.

The second largest background, from $t\bar{t}$ events, is assigned a 6% normalisation uncertainty corresponding to the uncertainty in the production cross-section. An additional uncertainty in the modelling of this background is derived from data/simulation differences observed in the top-quark p_T spectrum in $t\bar{t}$ differential cross-section measurements [67]. This uncertainty has an approxi-

mately linear dependence on m_{tb} . It is 13% at $m_{tb} = 1$ TeV, 31% at $m_{tb} = 2$ TeV, 48% at $m_{tb} = 3$ TeV and 65% at $m_{tb} = 4$ TeV.

The total systematic uncertainty in the background yield is dominated by uncertainties in the 2D sideband method and in the flavour-tagging efficiencies. The dominant systematic uncertainty in the signal yield is due to uncertainties in flavor tagging and top tagging efficiencies. The impact of theoretical uncertainties in the signal acceptance on the results of the analysis is negligible. The statistical uncertainty of the data dominates for $m_{tb} > 2$ TeV.

7. Statistical analysis and results

In order to test for the presence of a massive resonance, templates in the variable m_{tb} obtained from the simulated signal event samples and the background events estimated using data-driven methods and simulation, are fit to data, using a binned maximum-likelihood approach based on the RooStats framework [74,75]. The fits are performed simultaneously in the three signal regions (see Section 5). The background processes considered in the maximum-likelihood fit are the dominant multi-jet background and W/Z +jets, estimated together using the 2D sideband method (see Section 5), and $t\bar{t}$ events (see Table 2 for event yields).

The systematic uncertainties described in Section 6 may change the acceptance and shape of the m_{tb} distribution of both a potential W' -boson signal and the background processes, and are incorporated into the fit as nuisance parameters with log-normal constraints, with correlations across signal regions and signal and background processes taken into account. Some systematic uncertainties, such as those in the JES, affect the shapes of the histogram templates. These systematic uncertainties in the shapes are accounted for by introducing nuisance parameters α_k that describe the possible variation in the shapes of the histograms for each process k . A log-normal constraint with mean 0 and width 1 is applied to each of the parameters α_k . When performing the maximum-likelihood fit, all of the parameters α_k are allowed to vary.

The signal (s) and background (b) expectations are functions of the nuisance parameters $\vec{\theta}$. These functions are built such that the response of s and b to each θ is factorised from the nominal value (s_0) of the expected rate: $s(\vec{\theta}) = s_0 \times \prod v(\vec{\theta})$ where $v(\vec{\theta})$ describe the effect of variations in the nuisance parameters $\vec{\theta}$ and similarly for b .

The p -value p_b , representing the probability that the data is compatible with the background-only hypothesis, is estimated using the log-likelihood ratio (LLR) test statistic and evaluated using the asymptotic approximation [76]. In the absence of any significant excess above the expected background, upper limits at the 95% CL on the signal production cross-section times branching ratio are derived using the CL_s method [77]. Limits derived using

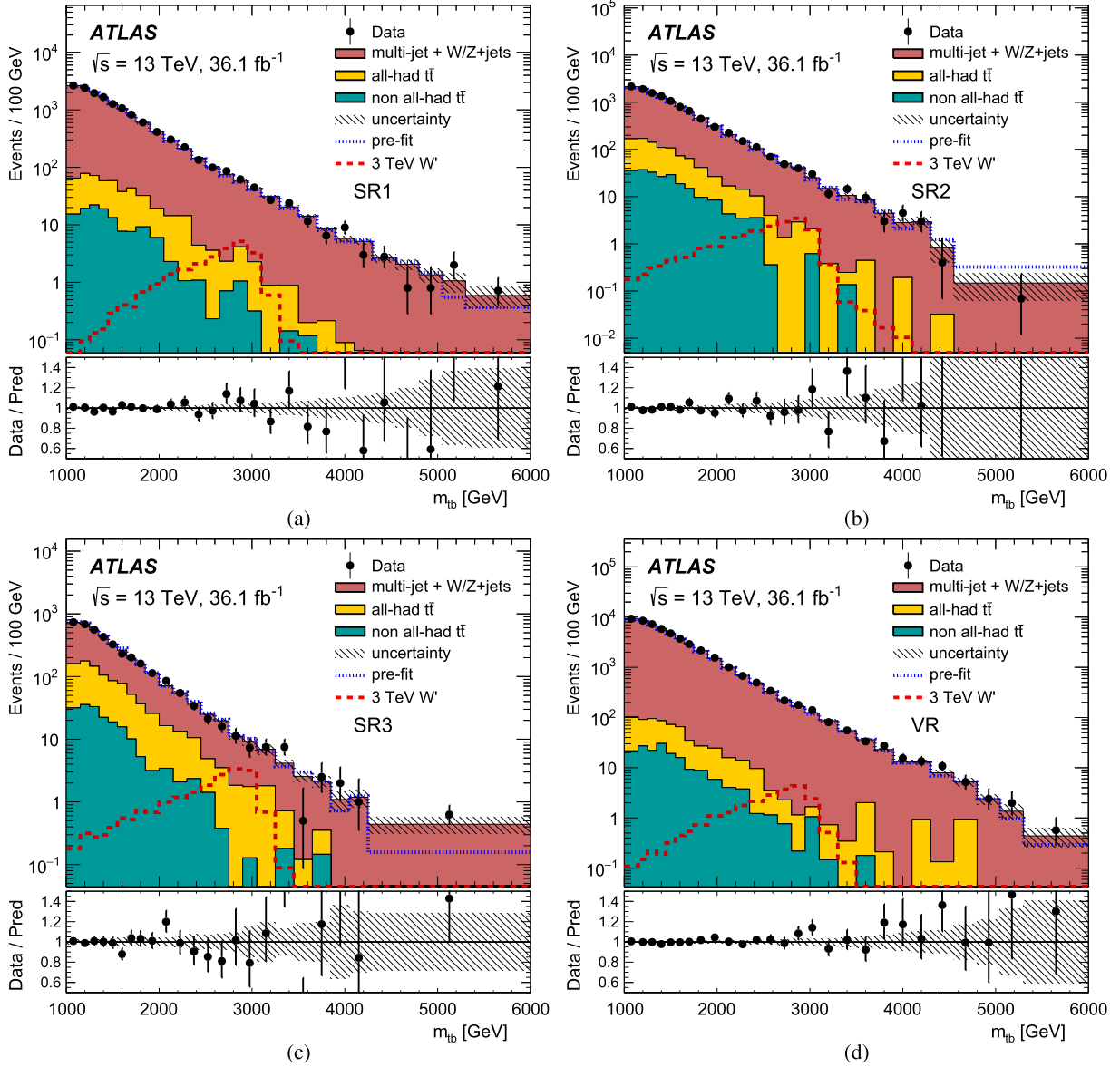


Fig. 4. Reconstructed $m_{t\bar{b}}$ distributions in data and for the background after the fit to data in the three signal regions and in the multi-jet validation region: (a) SR1, (b) SR2, (c) SR3, and (d) VR. The top panel shows the total-background $m_{t\bar{b}}$ distribution before the fit to data as the narrow dotted line and the 3 TeV W' -boson signal $m_{t\bar{b}}$ distribution as the dashed line. The “non all-had $t\bar{t}$ ” label refers to $t\bar{t}$ events in which the W boson from one or both top quarks decays leptonically. The bottom panel of the plot shows the ratio of data to prediction and the hatched band includes the systematic uncertainties after the fit to data.

the asymptotic approximation were cross-checked using pseudo-experiments and found to have a difference of less than 10% for all W' signal masses.

Fig. 4 shows the $m_{t\bar{b}}$ distributions in the three signal regions and the validation region after the fit to data. The fit in VR is done independently to test the post-fit agreement of the prediction with data. The maximum value of $m_{t\bar{b}}$ observed in data is 5.8 TeV. The hatched band in the bottom panel includes the systematic uncertainties described in Section 6 after the fit to data. The most discrepant region, at 2.25 TeV, has a local significance of 2.0σ for the combined fit in the three SRs, consistent with the background-only hypothesis. In the absence of any significant excess over the background-only hypothesis, 95% CL limits are derived on the cross-section times branching ratio of W' to $t\bar{b}$ decay, as shown in Fig. 5, for the right-handed and left-handed couplings. The observed and expected limits are derived using a linear interpolation between simulated signal mass hypotheses. They translate

to observed (expected) lower limits on the mass of a W' boson, with the same coupling to fermions as the SM W boson, of 3.0 (3.0) TeV and 2.9 (2.8) TeV in the right- and left-handed models, respectively. These mass limit values are obtained from the intersection of the theory curve and the observed and expected limit curves using a linear interpolation between the 2.75 TeV and 3 TeV W' -boson signal mass points. The narrow dotted curve in Fig. 5 shows the cross-section times branching ratio of W' to $t\bar{b}$ decay calculated with ZROP [15]. The band around this curve shows the uncertainty in the theoretical cross-section obtained by summing in quadrature the uncertainties in the estimation of the parton distribution function, strong coupling constant, renormalization and factorization scales and the top-quark mass. The difference between the mass exclusion limit results for W'_R - and W'_L -boson signals is mainly due to different total cross-sections ($\sigma(pp \rightarrow W') \cdot B(W' \rightarrow t\bar{b})$) of the two processes as discussed in Section 3.

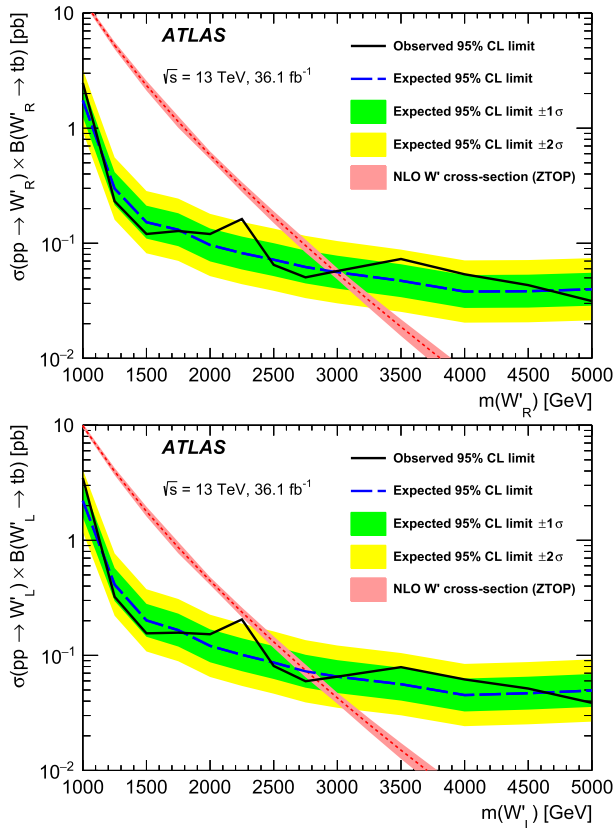


Fig. 5. Observed and expected 95% CL limits on the W'_R -boson (top) and W'_L -boson (bottom) cross-sections times branching ratio of W' to $t\bar{b}$ decay as a function of the corresponding W' -boson mass. The expected 95% CL limits are shown with ± 1 and ± 2 standard deviation (s.d.) bands. The narrow dotted curves show the theoretical cross-section predictions and the bands around them show the uncertainties in the predictions for the corresponding W' -boson signal. The observed and expected limits are derived using a linear interpolation between simulated signal mass hypotheses.

8. Summary

A search for $W' \rightarrow t\bar{b} \rightarrow q\bar{q}'b\bar{b}$ is presented using 36.1 fb^{-1} of $\sqrt{s} = 13 \text{ TeV}$ proton–proton collision data collected with the ATLAS detector at the LHC. The analysis makes use of jet substructure tagging optimised to select large- R jets originating from hadronically decaying top quarks using the shower deconstruction algorithm and b -tagging of small- R jets. The observed $m_{t\bar{b}}$ spectrum is consistent with the background-only prediction and exclusion limits at 95% CL are set on the W' -boson production cross-section times branching ratio to $t\bar{b}$ for right-handed and left-handed couplings as a function of the W' mass in the range 1–5 TeV. Cross-section limits are set at high W' -boson masses, excluding W' bosons with right-handed couplings with masses below 3.0 TeV and excluding W' bosons with left-handed couplings with masses below 2.9 TeV (at 95% CL).

Acknowledgements

We thank CERN for the very successful operation of the LHC, as well as the support staff from our institutions without whom ATLAS could not be operated efficiently.

We acknowledge the support of ANPCyT, Argentina; YerPhI, Armenia; ARC, Australia; BMWFW and FWF, Austria; ANAS, Azerbaijan; SSTC, Belarus; CNPq and FAPESP, Brazil; NSERC, NRC and CFI, Canada; CERN; CONICYT, Chile; CAS, MOST and NSFC, China; COLCIENCIAS, Colombia; MSMT CR, MPO CR and VSC CR, Czech

Republic; DNRF and DNSRC, Denmark; IN2P3-CNRS, CEA-DRF/IRFU, France; SRNSFG, Georgia; BMBF, HGF, and MPG, Germany; GSRT, Greece; RGC, Hong Kong SAR, China; ISF, I-CORE and Benozio Center, Israel; INFN, Italy; MEXT and JSPS, Japan; CNRST, Morocco; NWO, Netherlands; RCN, Norway; MNiSW and NCN, Poland; FCT, Portugal; MNE/IFA, Romania; MES of Russia and NRC KI, Russian Federation; JINR; MESTD, Serbia; MSSR, Slovakia; ARRS and MIZŠ, Slovenia; DST/NRF, South Africa; MINECO, Spain; SRC and Wallenberg Foundation, Sweden; SERI, SNSF and Cantons of Bern and Geneva, Switzerland; MOST, Taiwan; TAEK, Turkey; STFC, United Kingdom; DOE and NSF, United States of America. In addition, individual groups and members have received support from BCKDF, the Canada Council, Canarie, CRC, Compute Canada, FQRNT, and the Ontario Innovation Trust, Canada; EPLANET, ERC, ERDF, FP7, Horizon 2020 and Marie Skłodowska-Curie Actions, European Union; Investissements d'Avenir Labex and IDEX, ANR, Région Auvergne and Fondation Partager le Savoir, France; DFG and AvH Foundation, Germany; Herakleitos, Thales and Aristeia programmes co-financed by EU-ESF and the Greek NSRF; BSF, GIF and Minerva, Israel; BRF, Norway; CERCA Programme Generalitat de Catalunya, Generalitat Valenciana, Spain; the Royal Society and Leverhulme Trust, United Kingdom.

The crucial computing support from all WLCG partners is acknowledged gratefully, in particular from CERN, the ATLAS Tier-1 facilities at TRIUMF (Canada), NDGF (Denmark, Norway, Sweden), CC-IN2P3 (France), KIT/GridKA (Germany), INFN-CNAF (Italy), NL-T1 (Netherlands), PIC (Spain), ASGC (Taiwan), RAL (UK) and BNL (USA), the Tier-2 facilities worldwide and large non-WLCG resource providers. Major contributors of computing resources are listed in Ref. [78].

References

- [1] K.R. Dienes, E. Dudas, T. Gherghetta, Grand unification at intermediate mass scales through extra dimensions, *Nucl. Phys. B* 537 (1999) 47, arXiv:hep-ph/9806292.
- [2] S. Weinberg, Implications of dynamical symmetry breaking, *Phys. Rev. D* 13 (1976) 974, Erratum: *Phys. Rev. D* 19 (1979) 1277.
- [3] L. Susskind, Dynamics of spontaneous symmetry breaking in the Weinberg–Salam theory, *Phys. Rev. D* 20 (1979) 2619.
- [4] S. Dimopoulos, L. Susskind, Mass without scalars, *Nucl. Phys. B* 155 (1979) 237.
- [5] E. Eichten, K. Lane, Dynamical breaking of weak interaction symmetries, *Phys. Lett. B* 90 (1980) 125.
- [6] D.J. Muller, S. Nandi, Topflavor: a separate SU(2) for the third family, *Phys. Lett. B* 383 (1996) 345, arXiv:hep-ph/9602390.
- [7] N. Arkani-Hamed, A.G. Cohen, E. Katz, A.E. Nelson, The lightest higgs, *J. High Energy Phys.* 07 (2002) 034, arXiv:hep-ph/0206021.
- [8] R.S. Chivukula, B.A. Dobrescu, H. Georgi, C.T. Hill, Top quark seesaw theory of electroweak symmetry breaking, *Phys. Rev. D* 59 (1999) 075003, arXiv:hep-ph/9809470.
- [9] G. Burdman, B.A. Dobrescu, E. Pontón, Resonances from two universal extra dimensions, *Phys. Rev. D* 74 (2006) 075008, arXiv:hep-ph/0601186.
- [10] E. Malkawi, T.M. Tait, C.-P. Yuan, A model of strong flavor dynamics for the top quark, *Phys. Lett. B* 385 (1996) 304, arXiv:hep-ph/9603349.
- [11] J.C. Pati, A. Salam, Lepton number as the fourth “color”, *Phys. Rev. D* 10 (1974) 275.
- [12] C.T. Hill, Topcolor assisted technicolor, *Phys. Lett. B* 345 (1995) 483, arXiv:hep-ph/9411426.
- [13] B. Altarelli, G. Mele, M. Ruiz-Altaba, Searching for new heavy vector bosons in $p\bar{p}$ colliders, *Z. Phys. C* 45 (1989) 109, Erratum: *Z. Phys. C* 47 (1990) 676.
- [14] Z. Sullivan, Fully differential W' production and decay at next-to-leading order in QCD, *Phys. Rev. D* 66 (2002) 075011, arXiv:hep-ph/0207290.
- [15] D. Duffy, Z. Sullivan, Model independent reach for W' bosons at the LHC, *Phys. Rev. D* 86 (2012) 075018, arXiv:1208.4858 [hep-ph].
- [16] CDF Collaboration, Search for the production of narrow $t\bar{b}$ resonances in 1.9 fb^{-1} of $p\bar{p}$ collisions at $\sqrt{s} = 1.96 \text{ TeV}$, *Phys. Rev. Lett.* 103 (2009) 041801, arXiv:0902.3276 [hep-ex].
- [17] D0 Collaboration, Search for $W' \rightarrow t\bar{b}$ resonances with left- and right-handed couplings to fermions, *Phys. Lett. B* 699 (2011) 145, arXiv:1101.0806 [hep-ex].
- [18] CMS Collaboration, Search for heavy resonances decaying to a top quark and a bottom quark in the lepton+ jets final state in proton–proton collisions at 13 TeV, *Phys. Lett. B* 777 (2018) 39, arXiv:1708.08539 [hep-ex].

- [19] ATLAS Collaboration, Search for $W' \rightarrow t\bar{b}$ in the lepton plus jets final state in proton–proton collisions at a centre-of-mass energy of $\sqrt{s} = 8$ TeV with the ATLAS detector, Phys. Lett. B 743 (2015) 235, arXiv:1410.4103 [hep-ex].
- [20] CMS Collaboration, Search for a W' boson decaying to a bottom quark and a top quark in pp collisions at $\sqrt{s} = 7$ TeV, Phys. Lett. B 718 (2013) 1229, arXiv:1208.0956 [hep-ex].
- [21] CMS Collaboration, Search for $W' \rightarrow tb$ decays in the lepton + jets final state in pp collisions at $\sqrt{s} = 8$ TeV, J. High Energy Phys. 05 (2014) 108, arXiv:1402.2176 [hep-ex].
- [22] ATLAS Collaboration, Search for $W' \rightarrow tb \rightarrow qqbb$ decays in pp collisions at $\sqrt{s} = 8$ TeV with the ATLAS detector, Eur. Phys. J. C 75 (2015) 165, arXiv:1408.0886 [hep-ex].
- [23] ATLAS Collaboration, Search for a new heavy gauge boson resonance decaying into a lepton and missing transverse momentum in 36 fb^{-1} of pp collisions at $\sqrt{s} = 13$ TeV with the ATLAS experiment, arXiv:1706.04786 [hep-ex], 2017.
- [24] CMS Collaboration, Search for heavy gauge W' boson in events with an energetic lepton and large missing transverse momentum at $\sqrt{s} = 13$ TeV, Phys. Lett. B 770 (2017) 278, arXiv:1612.09274 [hep-ex].
- [25] ATLAS Collaboration, Identification of high transverse momentum top quarks in pp collisions at $\sqrt{s} = 8$ TeV with the ATLAS detector, J. High Energy Phys. 06 (2016) 093, arXiv:1603.03127 [hep-ex].
- [26] D.E. Soper, M. Spannowsky, Finding physics signals with shower deconstruction, Phys. Rev. D 84 (2011) 074002, arXiv:1102.3480 [hep-ph].
- [27] D.E. Soper, M. Spannowsky, Finding top quarks with shower deconstruction, Phys. Rev. D 87 (2013) 054012, arXiv:1211.3140 [hep-ph].
- [28] ATLAS Collaboration, The ATLAS experiment at the CERN large hadron collider, J. Instrum. 3 (2008) S08003.
- [29] ATLAS Collaboration, ATLAS insertable B-layer technical design report, ATLAS-TDR-19, <https://cds.cern.ch/record/1291633>, 2010, ATLAS insertable B-layer technical design report addendum, ATLAS-TDR-19-ADD-1, <https://cds.cern.ch/record/1451888>, 2012.
- [30] ATLAS Collaboration, Performance of the ATLAS trigger system in 2015, Eur. Phys. J. C 77 (2017) 317, arXiv:1611.09661 [hep-ex].
- [31] J. Alwall, et al., The automated computation of tree-level and next-to-leading order differential cross sections, and their matching to parton shower simulations, J. High Energy Phys. 07 (2014) 79, arXiv:1405.0301 [hep-ph].
- [32] T. Sjöstrand, S. Mrenna, P. Skands, A brief introduction to PYTHIA 8.1, Comput. Phys. Commun. 178 (2008) 852, arXiv:0710.3820 [hep-ph].
- [33] R.D. Ball, et al., A first unbiased global NLO determination of parton distributions and their uncertainties, Nucl. Phys. B 838 (2010) 136, arXiv:1002.4407 [hep-ph].
- [34] ATLAS Collaboration, ATLAS Pythia 8 tunes to 7 TeV data, ATL-PHYS-PUB-2014-021, <https://cds.cern.ch/record/1966419>, 2014.
- [35] M. Bahr, et al., Herwig++ physics and manual, Eur. Phys. J. C 58 (2008) 639, arXiv:0803.0883 [hep-ph].
- [36] T. Gleisberg, et al., Event generation with SHERPA 1.1, J. High Energy Phys. 02 (2009) 007, arXiv:0811.4622 [hep-ph].
- [37] S. Alioli, P. Nason, C. Oleari, E. Re, A general framework for implementing NLO calculations in shower Monte Carlo programs: the POWHEG BOX, J. High Energy Phys. 06 (2010) 043, arXiv:1002.2581 [hep-ph].
- [38] S. Frixione, P. Nason, G. Ridolfi, A positive-weight next-to-leading-order Monte Carlo for heavy flavour hadroproduction, J. High Energy Phys. 09 (2007) 126, arXiv:0707.3088 [hep-ph].
- [39] G. Corcella, et al., HERWIG 6: an event generator for hadron emission reactions with interfering gluons (including supersymmetric processes), J. High Energy Phys. 01 (2001) 010, arXiv:hep-ph/0011363.
- [40] H.-L. Lai, et al., New parton distributions for collider physics, Phys. Rev. D 82 (2010) 074024, arXiv:1007.2241 [hep-ph].
- [41] M. Cacciari, M. Czakon, M. Mangano, A. Mitov, P. Nason, Top-pair production at hadron colliders with next-to-next-to-leading logarithmic soft-gluon resummation, Phys. Lett. B 710 (2012) 612, arXiv:1111.5869 [hep-ph].
- [42] M. Beneke, P. Falgari, S. Klein, C. Schwinn, Hadronic top-quark pair production with NNLL threshold resummation, Nucl. Phys. B 855 (2012) 695, arXiv:1109.1536 [hep-ph].
- [43] P. Bärnreuther, M. Czakon, A. Mitov, Percent-level-precision physics at the tevatron: next-to-next-to-leading order QCD corrections to $q\bar{q} \rightarrow t\bar{t} + X$, Phys. Rev. Lett. 109 (2012) 132001, arXiv:1204.5201 [hep-ph].
- [44] M. Czakon, P. Fiedler, A. Mitov, Total top-quark pair-production cross section at hadron colliders through $O(\alpha_s^3)$, Phys. Rev. Lett. 110 (2013) 252004, arXiv:1303.6254 [hep-ph].
- [45] M. Czakon, A. Mitov, NNLO corrections to top pair production at hadron colliders: the quark–gluon reaction, J. High Energy Phys. 01 (2013) 080, arXiv:1210.6832 [hep-ph].
- [46] M. Czakon, A. Mitov, NNLO corrections to top-pair production at hadron colliders: the all-fermionic scattering channels, J. High Energy Phys. 12 (2012) 054, arXiv:1207.0236 [hep-ph].
- [47] M. Czakon, A. Mitov, Top++: a program for the calculation of the top-pair cross-section at hadron colliders, Comput. Phys. Commun. 185 (2014) 2930, arXiv:1112.5675 [hep-ph].
- [48] T. Sjöstrand, et al., High-energy physics event generation with PYTHIA 6.1, Comput. Phys. Commun. 135 (2001) 238, arXiv:hep-ph/0010017.
- [49] P.Z. Skands, Tuning Monte Carlo generators: the Perugia tunes, Phys. Rev. D 82 (2010) 074018, arXiv:1005.3457 [hep-ph].
- [50] D. Lange, The EvtGen particle decay simulation package, Nucl. Instrum. Methods A 462 (2001) 152.
- [51] S. Agostinelli, et al., GEANT4 – a simulation toolkit, Nucl. Instrum. Methods A 506 (2003) 250.
- [52] ATLAS Collaboration, The ATLAS simulation infrastructure, Eur. Phys. J. C 70 (2010) 823, arXiv:1005.4568 [physics.ins-det].
- [53] M. Cacciari, G.P. Salam, G. Soyez, The anti- k_t jet clustering algorithm, J. High Energy Phys. 04 (2008) 063, arXiv:0802.1189 [hep-ph].
- [54] M. Cacciari, G.P. Salam, G. Soyez, FastJet user manual, Eur. Phys. J. C 72 (2012) 1896, arXiv:1111.6097 [hep-ph].
- [55] ATLAS Collaboration, Jet calibration and systematic uncertainties for jets reconstructed in the ATLAS detector at $\sqrt{s} = 13$ TeV, ATL-PHYS-PUB-2015-015, <https://cds.cern.ch/record/2037613>, 2015.
- [56] ATLAS Collaboration, Identification and rejection of pile-up jets at high pseudorapidity with the ATLAS detector, Eur. Phys. J. C 77 (2017) 580, arXiv:1705.02211 [hep-ex].
- [57] D. Krohn, J. Thaler, L.-T. Wang, Jet trimming, J. High Energy Phys. 02 (2010) 084, arXiv:0912.1342 [hep-ph].
- [58] S. Catani, Y. Dokshitzer, M. Seymour, B. Webber, Longitudinally-invariant k_t -clustering algorithms for hadron–hadron collisions, Nucl. Phys. B 406 (1993) 187.
- [59] S. Ellis, D. Soper, Successive combination jet algorithm for hadron collisions, Phys. Rev. D 48 (1993) 3160, arXiv:hep-ph/9305266.
- [60] ATLAS Collaboration, Jet mass reconstruction with the ATLAS detector in early Run 2 data, ATLAS-CONF-2016-035, <https://cds.cern.ch/record/2200211>, 2016.
- [61] ATLAS Collaboration, Performance of pile-up mitigation techniques for jets in pp collisions at $\sqrt{s} = 8$ TeV using the ATLAS detector, Eur. Phys. J. C 76 (2016) 581, arXiv:1510.03823 [hep-ex].
- [62] ATLAS Collaboration, Performance of b -jet identification in the ATLAS experiment, J. Instrum. 11 (2016) P04008, arXiv:1512.01094 [hep-ex].
- [63] ATLAS Collaboration, Optimisation of the ATLAS b -tagging performance for the 2016 LHC Run, ATL-PHYS-PUB-2016-012, <https://cds.cern.ch/record/2160731>, 2016.
- [64] ATLAS Collaboration, Expected performance of the ATLAS b -tagging algorithms in Run-2, ATL-PHYS-PUB-2015-022, <https://cds.cern.ch/record/2037697>, 2015.
- [65] ATLAS Collaboration, Electron efficiency measurements with the ATLAS detector using 2012 LHC proton–proton collision data, Eur. Phys. J. C 77 (2017) 195, arXiv:1612.01456 [hep-ex].
- [66] ATLAS Collaboration, Muon reconstruction performance of the ATLAS detector in proton–proton collision data at $\sqrt{s} = 13$ TeV, Eur. Phys. J. C 76 (2016) 292, arXiv:1603.05598 [hep-ex].
- [67] ATLAS Collaboration, Measurements of top-quark pair differential cross-sections in the lepton+jets channel in pp collisions at $\sqrt{s} = 13$ TeV using the ATLAS detector, J. High Energy Phys. 11 (2017) 191, arXiv:1708.00727 [hep-ex].
- [68] M. Cacciari, G.P. Salam, G. Soyez, The catchment area of jets, J. High Energy Phys. 04 (2008) 005, arXiv:0802.1188 [hep-ph].
- [69] J.M. Butterworth, A.R. Davison, M. Rubin, G.P. Salam, Jet substructure as a new higgs- search channel at the large hadron collider, Phys. Rev. Lett. 100 (2008) 242001.
- [70] ATLAS Collaboration, Boosted object tagging with variable- R jets in the ATLAS detector, ATL-PHYS-PUB-2016-013, <https://cds.cern.ch/record/2199360>, 2016.
- [71] ATLAS Collaboration, Jet energy scale measurements and their systematic uncertainties in proton–proton collisions at $\sqrt{s} = 13$ TeV with the ATLAS detector, Phys. Rev. D 96 (2017) 072002, arXiv:1703.09665 [hep-ex].
- [72] ATLAS Collaboration, Jet global sequential corrections with the ATLAS detector in proton–proton collisions at $\sqrt{s} = 8$ TeV, ATLAS-CONF-2015-002, <https://cds.cern.ch/record/2001682>, 2015.
- [73] ATLAS Collaboration, Luminosity determination in pp collisions at $\sqrt{s} = 8$ TeV using the ATLAS detector at the LHC, Eur. Phys. J. C 76 (2016) 653, arXiv:1608.03953 [hep-ex].
- [74] L. Moneta, The RooStats project, in: Proceedings of Science, 2010, arXiv:1009.1003 [hep-ph].
- [75] M. Baak, et al., HistFitter software framework for statistical data analysis, Eur. Phys. J. C 75 (2015) 153, arXiv:1410.1280 [hep-ex].
- [76] G. Cowan, K. Cranmer, E. Gross, O. Vitells, Asymptotic formulae for likelihood-based tests of new physics, Eur. Phys. J. C 71 (2011) 1554, arXiv:1007.1727 [physics.data-an], Erratum: Eur. Phys. J. C 73 (2013) 2501.
- [77] A.L. Read, Presentation of search results: the CL_s technique, J. Phys. G 28 (2002) 2693.
- [78] ATLAS Collaboration, ATLAS computing acknowledgements 2016–2017, ATL-GEN-PUB-2016-002, <https://cds.cern.ch/record/2202407>.

The ATLAS Collaboration

M. Aaboud ^{137d}, G. Aad ⁸⁸, B. Abbott ¹¹⁵, O. Abidinov ^{12,*}, B. Abeloos ¹¹⁹, S.H. Abidi ¹⁶¹, O.S. AbouZeid ¹³⁹, N.L. Abraham ¹⁵¹, H. Abramowicz ¹⁵⁵, H. Abreu ¹⁵⁴, Y. Abulaiti ⁶, B.S. Acharya ^{167a,167b,a}, S. Adachi ¹⁵⁷, L. Adamczyk ^{41a}, J. Adelman ¹¹⁰, M. Adersberger ¹⁰², A. Adiguzel ^{20a}, T. Adye ¹³³, A.A. Affolder ¹³⁹, Y. Afik ¹⁵⁴, C. Agheorghiesei ^{28c}, J.A. Aguilar-Saavedra ^{128a,128f}, S.P. Ahlen ²⁴, F. Ahmadov ^{68,b}, G. Aielli ^{135a,135b}, S. Akatsuka ⁷¹, T.P.A. Åkesson ⁸⁴, E. Akilli ⁵², A.V. Akimov ⁹⁸, G.L. Alberghi ^{22a,22b}, J. Albert ¹⁷², P. Albicocco ⁵⁰, M.J. Alconada Verzini ⁷⁴, S. Alderweireldt ¹⁰⁸, M. Aleksa ³², I.N. Aleksandrov ⁶⁸, C. Alexa ^{28b}, G. Alexander ¹⁵⁵, T. Alexopoulos ¹⁰, M. Alhroob ¹¹⁵, B. Ali ¹³⁰, M. Aliev ^{76a,76b}, G. Alimonti ^{94a}, J. Alison ³³, S.P. Alkire ¹⁴⁰, C. Allaire ¹¹⁹, B.M.M. Allbrooke ¹⁵¹, B.W. Allen ¹¹⁸, P.P. Allport ¹⁹, A. Aloisio ^{106a,106b}, A. Alonso ³⁹, F. Alonso ⁷⁴, C. Alpigiani ¹⁴⁰, A.A. Alshehri ⁵⁶, M.I. Alstary ⁸⁸, B. Alvarez Gonzalez ³², D. Álvarez Piqueras ¹⁷⁰, M.G. Alvigi ^{106a,106b}, B.T. Amadio ¹⁶, Y. Amaral Coutinho ^{26a}, L. Ambroz ¹²², C. Amelung ²⁵, D. Amidei ⁹², S.P. Amor Dos Santos ^{128a,128c}, S. Amoroso ³², C.S. Amrouche ⁵², C. Anastopoulos ¹⁴¹, L.S. Ancu ⁵², N. Andari ¹⁹, T. Andeen ¹¹, C.F. Anders ^{60b}, J.K. Anders ¹⁸, K.J. Anderson ³³, A. Andreazza ^{94a,94b}, V. Andrei ^{60a}, S. Angelidakis ³⁷, I. Angelozzi ¹⁰⁹, A. Angerami ³⁸, A.V. Anisenkov ^{111,c}, A. Annovi ^{126a}, C. Antel ^{60a}, M.T. Anthony ¹⁴¹, M. Antonelli ⁵⁰, D.J.A. Antrim ¹⁶⁶, F. Anulli ^{134a}, M. Aoki ⁶⁹, L. Aperio Bella ³², G. Arabidze ⁹³, Y. Arai ⁶⁹, J.P. Araque ^{128a}, V. Araujo Ferraz ^{26a}, R. Araujo Pereira ^{26a}, A.T.H. Arce ⁴⁸, R.E. Ardell ⁸⁰, F.A. Arduh ⁷⁴, J-F. Arguin ⁹⁷, S. Argyropoulos ⁶⁶, A.J. Armbruster ³², L.J. Armitage ⁷⁹, O. Arnaez ¹⁶¹, H. Arnold ¹⁰⁹, M. Arratia ³⁰, O. Arslan ²³, A. Artamonov ^{99,*}, G. Artoni ¹²², S. Artz ⁸⁶, S. Asai ¹⁵⁷, N. Asbah ⁴⁵, A. Ashkenazi ¹⁵⁵, E.M. Asimakopoulou ¹⁶⁸, L. Asquith ¹⁵¹, K. Assamagan ²⁷, R. Astalos ^{146a}, R.J. Atkin ^{147a}, M. Atkinson ¹⁶⁹, N.B. Atlay ¹⁴³, K. Augsten ¹³⁰, G. Avolio ³², R. Avramidou ^{36a}, B. Axen ¹⁶, M.K. Ayoub ^{35a}, G. Azuelos ^{97,d}, A.E. Baas ^{60a}, M.J. Baca ¹⁹, H. Bachacou ¹³⁸, K. Bachas ^{76a,76b}, M. Backes ¹²², P. Bagnaia ^{134a,134b}, M. Bahmani ⁴², H. Bahrasemani ¹⁴⁴, A.J. Bailey ¹⁷⁰, J.T. Baines ¹³³, M. Bajic ³⁹, O.K. Baker ¹⁷⁹, P.J. Bakker ¹⁰⁹, D. Bakshi Gupta ⁸², E.M. Baldin ^{111,c}, P. Balek ¹⁷⁵, F. Balli ¹³⁸, W.K. Balunas ¹²⁴, E. Banas ⁴², A. Bandyopadhyay ²³, Sw. Banerjee ^{176,e}, A.A.E. Bannoura ¹⁷⁷, L. Barak ¹⁵⁵, W.M. Barbe ³⁷, E.L. Barberio ⁹¹, D. Barberis ^{53a,53b}, M. Barbero ⁸⁸, T. Barillari ¹⁰³, M-S Barisits ³², J.T. Barkeloo ¹¹⁸, T. Barklow ¹⁴⁵, N. Barlow ³⁰, R. Barnea ¹⁵⁴, S.L. Barnes ^{36c}, B.M. Barnett ¹³³, R.M. Barnett ¹⁶, Z. Barnovska-Blenessy ^{36a}, A. Baroncelli ^{136a}, G. Barone ²⁵, A.J. Barr ¹²², L. Barranco Navarro ¹⁷⁰, F. Barreiro ⁸⁵, J. Barreiro Guimarães da Costa ^{35a}, R. Bartoldus ¹⁴⁵, A.E. Barton ⁷⁵, P. Bartos ^{146a}, A. Basalae ¹²⁵, A. Bassalat ^{119,f}, R.L. Bates ⁵⁶, S.J. Batista ¹⁶¹, S. Batlamous ^{137e}, J.R. Batley ³⁰, M. Battaglia ¹³⁹, M. Bauce ^{134a,134b}, F. Bauer ¹³⁸, K.T. Bauer ¹⁶⁶, H.S. Bawa ^{145,g}, J.B. Beacham ¹¹³, M.D. Beattie ⁷⁵, T. Beau ⁸³, P.H. Beauchemin ¹⁶⁵, P. Bechtel ²³, H.P. Beck ^{18,h}, H.C. Beck ⁵⁸, K. Becker ⁵¹, M. Becker ⁸⁶, C. Becot ¹¹², A.J. Beddall ^{20e}, A. Beddall ^{20b}, V.A. Bednyakov ⁶⁸, M. Bedognetti ¹⁰⁹, C.P. Bee ¹⁵⁰, T.A. Beermann ³², M. Begalli ^{26a}, M. Begel ²⁷, A. Behera ¹⁵⁰, J.K. Behr ⁴⁵, A.S. Bell ⁸¹, G. Bella ¹⁵⁵, L. Bellagamba ^{22a}, A. Bellerive ³¹, M. Bellomo ¹⁵⁴, K. Belotskiy ¹⁰⁰, N.L. Belyaev ¹⁰⁰, O. Benary ^{155,*}, D. Benchekrone ^{137a}, M. Bender ¹⁰², N. Benekos ¹⁰, Y. Benhammou ¹⁵⁵, E. Benhar Noccioli ¹⁷⁹, J. Benitez ⁶⁶, D.P. Benjamin ⁴⁸, M. Benoit ⁵², J.R. Bensinger ²⁵, S. Bentvelsen ¹⁰⁹, L. Beresford ¹²², M. Beretta ⁵⁰, D. Berge ⁴⁵, E. Bergeaas Kuutmann ¹⁶⁸, N. Berger ⁵, L.J. Bergsten ²⁵, J. Beringer ¹⁶, S. Berlendis ⁵⁷, N.R. Bernard ⁸⁹, G. Bernardi ⁸³, C. Bernius ¹⁴⁵, F.U. Bernlochner ²³, T. Berry ⁸⁰, P. Berta ⁸⁶, C. Bertella ^{35a}, G. Bertoli ^{148a,148b}, I.A. Bertram ⁷⁵, G.J. Besjes ³⁹, O. Bessidskaia Bylund ^{148a,148b}, M. Bessner ⁴⁵, N. Besson ¹³⁸, A. Bethani ⁸⁷, S. Bethke ¹⁰³, A. Betti ²³, A.J. Bevan ⁷⁹, J. Beyer ¹⁰³, R.M. Bianchi ¹²⁷, O. Biebel ¹⁰², D. Biedermann ¹⁷, R. Bielski ⁸⁷, K. Bierwagen ⁸⁶, N.V. Biesuz ^{126a,126b}, M. Biglietti ^{136a}, T.R.V. Billoud ⁹⁷, M. Bindi ⁵⁸, A. Bingul ^{20b}, C. Bini ^{134a,134b}, S. Biondi ^{22a,22b}, T. Bisanz ⁵⁸, J.P. Biswal ¹⁵⁵, C. Bittrich ⁴⁷, D.M. Bjergaard ⁴⁸, J.E. Black ¹⁴⁵, K.M. Black ²⁴, R.E. Blair ⁶, T. Blazek ^{146a}, I. Bloch ⁴⁵, C. Blocker ²⁵, A. Blue ⁵⁶, U. Blumenschein ⁷⁹, Dr. Blunier ^{34a}, G.J. Bobbink ¹⁰⁹, V.S. Bobrovnikov ^{111,c}, S.S. Bocchetta ⁸⁴, A. Bocci ⁴⁸, D. Boerner ¹⁷⁷, D. Bogavac ¹⁰², A.G. Bogdanchikov ¹¹¹, C. Boehm ^{148a}, V. Boisvert ⁸⁰, P. Bokan ^{168,i}, T. Bold ^{41a}, A.S. Boldyrev ¹⁰¹, A.E. Bolz ^{60b}, M. Bomben ⁸³, M. Bona ⁷⁹, J.S. Bonilla ¹¹⁸, M. Boonekamp ¹³⁸, A. Borisov ¹³², G. Borissov ⁷⁵, J. Bortfeldt ³², D. Bortoletto ¹²², V. Bortolotto ^{135a,135b}, D. Boscherini ^{22a}, M. Bosman ¹³, J.D. Bossio Sola ²⁹, J. Boudreau ¹²⁷, E.V. Bouhova-Thacker ⁷⁵, D. Boumediene ³⁷, C. Bourdarios ¹¹⁹, S.K. Boutle ⁵⁶, A. Boveia ¹¹³, J. Boyd ³², I.R. Boyko ⁶⁸, A.J. Bozson ⁸⁰, J. Bracinik ¹⁹, N. Brahimi ⁸⁸, A. Brandt ⁸, G. Brandt ¹⁷⁷, O. Brandt ^{60a}, F. Braren ⁴⁵, U. Bratzler ¹⁵⁸, B. Brau ⁸⁹, J.E. Brau ¹¹⁸, W.D. Breaden Madden ⁵⁶, K. Brendlinger ⁴⁵,

A.J. Brennan⁹¹, L. Brenner⁴⁵, R. Brenner¹⁶⁸, S. Bressler¹⁷⁵, B. Brickwedde⁸⁶, D.L. Briglin¹⁹, D. Britton⁵⁶,
 D. Britzger^{60b}, I. Brock²³, R. Brock⁹³, G. Brooijmans³⁸, T. Brooks⁸⁰, W.K. Brooks^{34b}, E. Brost¹¹⁰,
 J.H. Broughton¹⁹, P.A. Bruckman de Renstrom⁴², D. Bruncko^{146b}, A. Bruni^{22a}, G. Bruni^{22a}, L.S. Bruni¹⁰⁹,
 S. Bruno^{135a,135b}, B.H. Brunt³⁰, M. Bruschi^{22a}, N. Brusino¹²⁷, P. Bryant³³, L. Bryngemark⁴⁵,
 T. Buanes¹⁵, Q. Buat³², P. Buchholz¹⁴³, A.G. Buckley⁵⁶, I.A. Budagov⁶⁸, F. Buehrer⁵¹, M.K. Bugge¹²¹,
 O. Bulekov¹⁰⁰, D. Bullock⁸, T.J. Burch¹¹⁰, S. Burdin⁷⁷, C.D. Burgard¹⁰⁹, A.M. Burger⁵, B. Burghgrave¹¹⁰,
 K. Burka⁴², S. Burke¹³³, I. Burmeister⁴⁶, J.T.P. Burr¹²², D. Büscher⁵¹, V. Büscher⁸⁶, E. Buschmann⁵⁸,
 P. Bussey⁵⁶, J.M. Butler²⁴, C.M. Buttar⁵⁶, J.M. Butterworth⁸¹, P. Butti³², W. Buttinger³², A. Buzatu¹⁵³,
 A.R. Buzykaev^{111,c}, G. Cabras^{22a,22b}, S. Cabrera Urbán¹⁷⁰, D. Caforio¹³⁰, H. Cai¹⁶⁹, V.M.M. Cairo²,
 O. Cakir^{4a}, N. Calace⁵², P. Calafiura¹⁶, A. Calandri⁸⁸, G. Calderini⁸³, P. Calfayan⁶⁴, G. Callea^{40a,40b},
 L.P. Caloba^{26a}, S. Calvente Lopez⁸⁵, D. Calvet³⁷, S. Calvet³⁷, T.P. Calvet¹⁵⁰, M. Calvetti^{126a,126b},
 R. Camacho Toro⁸³, S. Camarda³², P. Camarri^{135a,135b}, D. Cameron¹²¹, R. Caminal Armadans⁸⁹,
 C. Camincher³², S. Campana³², M. Campanelli⁸¹, A. Camplani^{94a,94b}, A. Campoverde¹⁴³,
 V. Canale^{106a,106b}, M. Cano Bret^{36c}, J. Cantero¹¹⁶, T. Cao¹⁵⁵, Y. Cao¹⁶⁹, M.D.M. Capeans Garrido³²,
 I. Caprini^{28b}, M. Caprini^{28b}, M. Capua^{40a,40b}, R.M. Carbone³⁸, R. Cardarelli^{135a}, F. Cardillo⁵¹, I. Carli¹³¹,
 T. Carli³², G. Carlino^{106a}, B.T. Carlson¹²⁷, L. Carminati^{94a,94b}, R.M.D. Carney^{148a,148b}, S. Caron¹⁰⁸,
 E. Carquin^{34b}, S. Carrá^{94a,94b}, G.D. Carrillo-Montoya³², D. Casadei^{147b}, M.P. Casado^{13,j}, A.F. Casha¹⁶¹,
 M. Casolino¹³, D.W. Casper¹⁶⁶, R. Castelijm¹⁰⁹, V. Castillo Gimenez¹⁷⁰, N.F. Castro^{128a,128e},
 A. Catinaccio³², J.R. Catmore¹²¹, A. Cattai³², J. Caudron²³, V. Cavaliere²⁷, E. Cavallaro¹³, D. Cavalli^{94a},
 M. Cavalli-Sforza¹³, V. Cavasinni^{126a,126b}, E. Celebi^{20d}, F. Ceradini^{136a,136b}, L. Cerda Alberich¹⁷⁰,
 A.S. Cerqueira^{26b}, A. Cerri¹⁵¹, L. Cerrito^{135a,135b}, F. Cerutti¹⁶, A. Cervelli^{22a,22b}, S.A. Cetin^{20d},
 A. Chafaq^{137a}, DC Chakraborty¹¹⁰, S.K. Chan⁵⁹, W.S. Chan¹⁰⁹, Y.L. Chan^{62a}, P. Chang¹⁶⁹, J.D. Chapman³⁰,
 D.G. Charlton¹⁹, C.C. Chau³¹, C.A. Chavez Barajas¹⁵¹, S. Che¹¹³, A. Chegwiddden⁹³, S. Chekanov⁶,
 S.V. Chekulaev^{163a}, G.A. Chelkov^{68,k}, M.A. Chelstowska³², C. Chen^{36a}, C. Chen⁶⁷, H. Chen²⁷, J. Chen^{36a},
 J. Chen³⁸, S. Chen^{35b}, S. Chen¹²⁴, X. Chen^{35c,l}, Y. Chen⁷⁰, Y.-H. Chen⁴⁵, H.C. Cheng⁹², H.J. Cheng^{35a,35d},
 A. Cheplakov⁶⁸, E. Cheremushkina¹³², R. Cherkaoui El Moursli^{137e}, E. Cheu⁷, K. Cheung⁶³,
 L. Chevalier¹³⁸, V. Chiarella⁵⁰, G. Chiarelli^{126a}, G. Chiodini^{76a}, A.S. Chisholm³², A. Chitan^{28b}, I. Chiu¹⁵⁷,
 Y.H. Chiu¹⁷², M.V. Chizhov⁶⁸, K. Choi⁶⁴, A.R. Chomont¹¹⁹, S. Chouridou¹⁵⁶, Y.S. Chow¹⁰⁹,
 V. Christodoulou⁸¹, M.C. Chu^{62a}, J. Chudoba¹²⁹, A.J. Chuinard⁹⁰, J.J. Chwastowski⁴², L. Chytka¹¹⁷,
 D. Cinca⁴⁶, V. Cindro⁷⁸, I.A. Cioară²³, A. Ciocio¹⁶, F. Ciotto^{106a,106b}, Z.H. Citron¹⁷⁵, M. Citterio^{94a},
 A. Clark⁵², M.R. Clark³⁸, P.J. Clark⁴⁹, C. Clement^{148a,148b}, Y. Coadou⁸⁸, M. Cokal^{167a,167c},
 A. Coccaro^{53a,53b}, J. Cochran⁶⁷, A.E.C. Coimbra¹⁷⁵, L. Colasurdo¹⁰⁸, B. Cole³⁸, A.P. Colijn¹⁰⁹, J. Collot⁵⁷,
 P. Conde Muiño^{128a,128b}, E. Coniavitis⁵¹, S.H. Connell^{147b}, I.A. Connelly⁸⁷, S. Constantinescu^{28b},
 F. Conventi^{106a,m}, A.M. Cooper-Sarkar¹²², F. Cormier¹⁷¹, K.J.R. Cormier¹⁶¹, M. Corradi^{134a,134b},
 E.E. Corrigan⁸⁴, F. Corriveau^{90,n}, A. Cortes-Gonzalez³², M.J. Costa¹⁷⁰, D. Costanzo¹⁴¹, G. Cottin³⁰,
 G. Cowan⁸⁰, B.E. Cox⁸⁷, J. Crane⁸⁷, K. Cranmer¹¹², S.J. Crawley⁵⁶, R.A. Creager¹²⁴, G. Cree³¹,
 S. Crépe-Renaudin⁵⁷, F. Crescioli⁸³, M. Cristinziani²³, V. Croft¹¹², G. Crosetti^{40a,40b}, A. Cueto⁸⁵,
 T. Cuhadar Donszelmann¹⁴¹, A.R. Cukierman¹⁴⁵, M. Curatolo⁵⁰, J. Cúth⁸⁶, S. Czekierda⁴²,
 P. Czodrowski³², G. D'amen^{22a,22b}, S. D'Auria⁵⁶, L. D'Eramo⁸³, M. D'Onofrio⁷⁷,
 M.J. Da Cunha Sargedas De Sousa^{36b,ba}, C. Da Via⁸⁷, W. Dabrowski^{41a}, T. Dado^{146a,i}, S. Dahbi^{137e},
 T. Dai⁹², F. Dallaire⁹⁷, C. Dallapiccola⁸⁹, M. Dam³⁹, J.R. Dandoy¹²⁴, M.F. Daneri²⁹, N.P. Dang^{176,e},
 N.D. Dann⁸⁷, M. Danninger¹⁷¹, V. Dao³², G. Darbo^{53a}, S. Darmora⁸, O. Dartsis⁵, A. Dattagupta¹¹⁸,
 T. Daubney⁴⁵, W. Davey²³, C. David⁴⁵, T. Davidek¹³¹, D.R. Davis⁴⁸, E. Dawe⁹¹, I. Dawson¹⁴¹, K. De⁸,
 R. de Asmundis^{106a}, A. De Benedetti¹¹⁵, S. De Castro^{22a,22b}, S. De Cecco^{134a,134b}, N. De Groot¹⁰⁸,
 P. de Jong¹⁰⁹, H. De la Torre⁹³, F. De Lorenzi⁶⁷, A. De Maria^{58,az}, D. De Pedis^{134a}, A. De Salvo^{134a},
 U. De Sanctis^{135a,135b}, A. De Santo¹⁵¹, K. De Vasconcelos Corga⁸⁸, J.B. De Vivie De Regie¹¹⁹,
 C. Debenedetti¹³⁹, D.V. Dedovich⁶⁸, N. Dehghanian³, M. Del Gaudio^{40a,40b}, J. Del Peso⁸⁵, D. Delgove¹¹⁹,
 F. Deliot¹³⁸, C.M. Delitzsch⁷, A. Dell'Acqua³², L. Dell'Asta²⁴, M. Della Pietra^{106a,106b}, D. della Volpe⁵²,
 M. Delmastro⁵, C. Delporte¹¹⁹, P.A. Delsart⁵⁷, D.A. DeMarco¹⁶¹, S. Demers¹⁷⁹, M. Demichev⁶⁸,
 S.P. Denisov¹³², D. Denysiuk¹⁰⁹, D. Derendarz⁴², J.E. Derkaoui^{137d}, F. Derue⁸³, P. Dervan⁷⁷, K. Desch²³,
 C. Deterre⁴⁵, K. Dette¹⁶¹, M.R. Devesa²⁹, P.O. Deviveiros³², A. Dewhurst¹³³, S. Dhaliwal²⁵,
 F.A. Di Bello⁵², A. Di Ciaccio^{135a,135b}, L. Di Ciaccio⁵, W.K. Di Clemente¹²⁴, C. Di Donato^{106a,106b},

A. Di Girolamo³², B. Di Micco^{136a,136b}, R. Di Nardo³², K.F. Di Petrillo⁵⁹, A. Di Simone⁵¹, R. Di Sipio¹⁶¹,
 D. Di Valentino³¹, C. Diaconu⁸⁸, M. Diamond¹⁶¹, F.A. Dias³⁹, T. Dias do Vale^{128a}, M.A. Diaz^{34a},
 J. Dickinson¹⁶, E.B. Diehl⁹², J. Dietrich¹⁷, S. Díez Cornell⁴⁵, A. Dimitrievska¹⁶, J. Dingfelder²³,
 F. Dittus³², F. Djama⁸⁸, T. Djobava^{54b}, J.I. Djuvsland^{60a}, M.A.B. do Vale^{26c}, M. Dobre^{28b},
 D. Dodsworth²⁵, C. Doglioni⁸⁴, J. Dolejsi¹³¹, Z. Dolezal¹³¹, M. Donadelli^{26d}, J. Donini³⁷, J. Dopke¹³³,
 A. Doria^{106a}, M.T. Dova⁷⁴, A.T. Doyle⁵⁶, E. Drechsler⁵⁸, E. Dreyer¹⁴⁴, T. Dreyer⁵⁸, M. Dris¹⁰, Y. Du^{36b},
 J. Duarte-Campderros¹⁵⁵, F. Dubinin⁹⁸, A. Dubreuil⁵², E. Duchovni¹⁷⁵, G. Duckeck¹⁰², A. Ducourthial⁸³,
 O.A. Ducu^{97,o}, D. Duda¹⁰³, A. Dudarev³², A.Chr. Dudder⁸⁶, E.M. Duffield¹⁶, L. Duflot¹¹⁹, M. Dührssen³²,
 C. Dülsen¹⁷⁷, M. Dumancic¹⁷⁵, A.E. Dumitriu^{28b,p}, A.K. Duncan⁵⁶, M. Dunford^{60a}, A. Duperrin⁸⁸,
 H. Duran Yildiz^{4a}, M. Düren⁵⁵, A. Durglishvili^{54b}, D. Duschinger⁴⁷, B. Dutta⁴⁵, D. Duvnjak¹,
 M. Dyndal⁴⁵, B.S. Dziedzic⁴², C. Eckardt⁴⁵, K.M. Ecker¹⁰³, R.C. Edgar⁹², T. Eifert³², G. Eigen¹⁵,
 K. Einsweiler¹⁶, T. Ekelof¹⁶⁸, M. El Kacimi^{137c}, R. El Kosseifi⁸⁸, V. Ellajosyula⁸⁸, M. Ellert¹⁶⁸,
 F. Ellinghaus¹⁷⁷, A.A. Elliot⁷⁹, N. Ellis³², J. Elmsheuser²⁷, M. Elsing³², D. Emelianov¹³³, Y. Enari¹⁵⁷,
 J.S. Ennis¹⁷³, M.B. Epland⁴⁸, J. Erdmann⁴⁶, A. Ereditato¹⁸, S. Errede¹⁶⁹, M. Escalier¹¹⁹, C. Escobar¹⁷⁰,
 B. Esposito⁵⁰, O. Estrada Pastor¹⁷⁰, A.I. Etiennev¹³⁸, E. Etzion¹⁵⁵, H. Evans⁶⁴, A. Ezhilov¹²⁵, M. Ezzi^{137e},
 F. Fabbri^{22a,22b}, L. Fabbri^{22a,22b}, V. Fabiani¹⁰⁸, G. Facini⁸¹, R.M. Faisca Rodrigues Pereira^{128a},
 R.M. Fakhruddinov¹³², S. Falciano^{134a}, P.J. Falke⁵, S. Falke⁵, J. Faltova¹³¹, Y. Fang^{35a}, M. Fanti^{94a,94b},
 A. Farbin⁸, A. Farilla^{136a}, E.M. Farina^{123a,123b}, T. Farooque⁹³, S. Farrell¹⁶, S.M. Farrington¹⁷³,
 P. Farthouat³², F. Fassi^{137e}, P. Fassnacht³², D. Fassoulotis⁹, M. Fauci Giannelli⁴⁹, A. Favareto^{53a,53b},
 W.J. Fawcett⁵², L. Fayard¹¹⁹, O.L. Fedin^{125,q}, W. Fedorko¹⁷¹, M. Feickert⁴³, S. Feigl¹²¹, L. Feligioni⁸⁸,
 C. Feng^{36b}, E.J. Feng³², M. Feng⁴⁸, M.J. Fenton⁵⁶, A.B. Fenyuk¹³², L. Feremenga⁸, J. Ferrando⁴⁵,
 A. Ferrari¹⁶⁸, P. Ferrari¹⁰⁹, R. Ferrari^{123a}, D.E. Ferreira de Lima^{60b}, A. Ferrer¹⁷⁰, D. Ferrere⁵²,
 C. Ferretti⁹², F. Fiedler⁸⁶, A. Filipčič⁷⁸, F. Filthaut¹⁰⁸, M. Fincke-Keeler¹⁷², K.D. Finelli²⁴,
 M.C.N. Fiolhais^{128a,128c,r}, L. Fiorini¹⁷⁰, C. Fischer¹³, W.C. Fisher⁹³, N. Flaschel⁴⁵, I. Fleck¹⁴³,
 P. Fleischmann⁹², R.R.M. Fletcher¹²⁴, T. Flick¹⁷⁷, B.M. Flierl¹⁰², L.M. Flores¹²⁴, L.R. Flores Castillo^{62a},
 N. Fomin¹⁵, G.T. Forcolin⁸⁷, A. Formica¹³⁸, F.A. Förster¹³, A.C. Forti⁸⁷, A.G. Foster¹⁹, D. Fournier¹¹⁹,
 H. Fox⁷⁵, S. Fracchia¹⁴¹, P. Francavilla^{126a,126b}, M. Franchini^{22a,22b}, S. Franchino^{60a}, D. Francis³²,
 L. Franconi¹²¹, M. Franklin⁵⁹, M. Frate¹⁶⁶, M. Fraternali^{123a,123b}, D. Freeborn⁸¹,
 S.M. Fressard-Batranceanu³², B. Freund⁹⁷, W.S. Freund^{26a}, D. Froidevaux³², J.A. Frost¹²², C. Fukunaga¹⁵⁸,
 T. Fusayasu¹⁰⁴, J. Fuster¹⁷⁰, O. Gabizon¹⁵⁴, A. Gabrielli^{22a,22b}, A. Gabrielli¹⁶, G.P. Gach^{41a},
 S. Gadatsch⁵², P. Gadow¹⁰³, G. Gagliardi^{53a,53b}, L.G. Gagnon⁹⁷, C. Galea^{28b}, B. Galhardo^{128a,128c},
 E.J. Gallas¹²², B.J. Gallop¹³³, P. Gallus¹³⁰, G. Galster³⁹, R. Gamboa Goni⁷⁹, K.K. Gan¹¹³, S. Ganguly¹⁷⁵,
 Y. Gao⁷⁷, Y.S. Gao^{145,g}, C. García¹⁷⁰, J.E. García Navarro¹⁷⁰, J.A. García Pascual^{35a}, M. Garcia-Sciveres¹⁶,
 R.W. Gardner³³, N. Garelli¹⁴⁵, V. Garonne¹²¹, K. Gasnikova⁴⁵, A. Gaudiello^{53a,53b}, G. Gaudio^{123a},
 I.L. Gavrilenko⁹⁸, A. Gavrilyuk⁹⁹, C. Gay¹⁷¹, G. Gaycken²³, E.N. Gazis¹⁰, C.N.P. Gee¹³³, J. Geisen⁵⁸,
 M. Geisen⁸⁶, M.P. Geisler^{60a}, K. Gellerstedt^{148a,148b}, C. Gemme^{53a}, M.H. Genest⁵⁷, C. Geng⁹²,
 S. Gentile^{134a,134b}, C. Gentsos¹⁵⁶, S. George⁸⁰, D. Gerbaudo¹³, G. Geßner⁴⁶, S. Ghasemi¹⁴³,
 M. Ghneimat²³, B. Giacobbe^{22a}, S. Giagu^{134a,134b}, N. Giangiacomi^{22a,22b}, P. Giannetti^{126a}, S.M. Gibson⁸⁰,
 M. Gignac¹³⁹, D. Gillberg³¹, G. Gilles¹⁷⁷, D.M. Gingrich^{3,d}, M.P. Giordani^{167a,167c}, F.M. Giorgi^{22a},
 P.F. Giraud¹³⁸, P. Giromini⁵⁹, G. Giugliarelli^{167a,167c}, D. Giugni^{94a}, F. Giuli¹²², M. Giulini^{60b},
 S. Gkaitatzis¹⁵⁶, I. Gkialas^{9,s}, E.L. Gkoukousis¹³, P. Gkoutoumis¹⁰, L.K. Gladilin¹⁰¹, C. Glasman⁸⁵,
 J. Glatzer¹³, P.C.F. Glaysher⁴⁵, A. Glazov⁴⁵, M. Goblirsch-Kolb²⁵, J. Godlewski⁴², S. Goldfarb⁹¹,
 T. Golling⁵², D. Golubkov¹³², A. Gomes^{128a,bb}, R. Gonçalves^{128a}, R. Goncalves Gama^{26b}, G. Gonella⁵¹,
 L. Gonella¹⁹, A. Gongadze⁶⁸, F. Gonnella¹⁹, J.L. Gonski⁵⁹, S. González de la Hoz¹⁷⁰,
 S. Gonzalez-Sevilla⁵², L. Goossens³², P.A. Gorbounov⁹⁹, H.A. Gordon²⁷, B. Gorini³², E. Gorini^{76a,76b},
 A. Gorišek⁷⁸, A.T. Goshaw⁴⁸, C. Gössling⁴⁶, M.I. Gostkin⁶⁸, C.A. Gottardo²³, C.R. Goudet¹¹⁹,
 D. Goujdami^{137c}, A.G. Goussiou¹⁴⁰, N. Govender^{147b,t}, C. Goy⁵, E. Gozani¹⁵⁴, I. Grabowska-Bold^{41a},
 P.O.J. Gradin¹⁶⁸, E.C. Graham⁷⁷, J. Gramling¹⁶⁶, E. Gramstad¹²¹, S. Grancagnolo¹⁷, V. Gratchev¹²⁵,
 P.M. Gravila^{28f}, C. Gray⁵⁶, H.M. Gray¹⁶, Z.D. Greenwood^{82,u}, C. Greife²³, K. Gregersen⁸¹, I.M. Gregor⁴⁵,
 P. Grenier¹⁴⁵, K. Grevtsov⁴⁵, J. Griffiths⁸, A.A. Grillo¹³⁹, K. Grimm¹⁴⁵, S. Grinstein^{13,v}, Ph. Gris³⁷,
 J.-F. Grivaz¹¹⁹, S. Groh⁸⁶, E. Gross¹⁷⁵, J. Grosse-Knetter⁵⁸, G.C. Grossi⁸², Z.J. Grout⁸¹, C. Grud⁹²,
 A. Grummer¹⁰⁷, L. Guan⁹², W. Guan¹⁷⁶, J. Guenther³², A. Guerguichon¹¹⁹, F. Guescini^{163a}, D. Guest¹⁶⁶,

R. Gugel⁵¹, B. Gui¹¹³, T. Guillemin⁵, S. Guindon³², U. Gul⁵⁶, C. Gumpert³², J. Guo^{36c}, W. Guo⁹², Y. Guo^{36a,w}, Z. Guo⁸⁸, R. Gupta⁴³, S. Gurbuz^{20a}, G. Gustavino¹¹⁵, B.J. Gutelman¹⁵⁴, P. Gutierrez¹¹⁵, C. Gutschew⁸¹, C. Guyot¹³⁸, M.P. Guzik^{41a}, C. Gwenlan¹²², C.B. Gwilliam⁷⁷, A. Hönle¹⁰³, A. Haas¹¹², C. Haber¹⁶, H.K. Hadavand⁸, N. Haddad^{137e}, A. Hadeef^{36a}, S. Hageböck²³, M. Hagihara¹⁶⁴, H. Hakobyan^{180,*}, M. Haleem¹⁷⁸, J. Haley¹¹⁶, G. Halladjian⁹³, G.D. Hallewell⁸⁸, K. Hamacher¹⁷⁷, P. Hamal¹¹⁷, K. Hamano¹⁷², A. Hamilton^{147a}, G.N. Hamity¹⁴¹, K. Han^{36a,x}, L. Han^{36a}, S. Han^{35a,35d}, K. Hanagaki^{69,y}, M. Hance¹³⁹, D.M. Handl¹⁰², B. Haney¹²⁴, R. Hankache⁸³, P. Hanke^{60a}, E. Hansen⁸⁴, J.B. Hansen³⁹, J.D. Hansen³⁹, M.C. Hansen²³, P.H. Hansen³⁹, K. Hara¹⁶⁴, A.S. Hard¹⁷⁶, T. Harenberg¹⁷⁷, S. Harkusha⁹⁵, P.F. Harrison¹⁷³, N.M. Hartmann¹⁰², Y. Hasegawa¹⁴², A. Hasib⁴⁹, S. Hassani¹³⁸, S. Haug¹⁸, R. Hauser⁹³, L. Hauswald⁴⁷, L.B. Havener³⁸, M. Havranek¹³⁰, C.M. Hawkes¹⁹, R.J. Hawking³², D. Hayden⁹³, C. Hayes¹⁵⁰, C.P. Hays¹²², J.M. Hays⁷⁹, H.S. Hayward⁷⁷, S.J. Haywood¹³³, M.P. Heath⁴⁹, V. Hedberg⁸⁴, L. Heelan⁸, S. Heer²³, K.K. Heidegger⁵¹, J. Heilman³¹, S. Heim⁴⁵, T. Heim¹⁶, B. Heinemann^{45,z}, J.J. Heinrich¹⁰², L. Heinrich¹¹², C. Heinz⁵⁵, J. Hejbal¹²⁹, L. Helary³², A. Held¹⁷¹, S. Hellesund¹²¹, S. Hellman^{148a,148b}, C. Helsens³², R.C.W. Henderson⁷⁵, Y. Heng¹⁷⁶, S. Henkelmann¹⁷¹, A.M. Henriques Correia³², G.H. Herbert¹⁷, H. Herde²⁵, V. Herget¹⁷⁸, Y. Hernández Jiménez^{147c}, H. Herr⁸⁶, G. Herten⁵¹, R. Hertenberger¹⁰², L. Hervas³², T.C. Herwig¹²⁴, G.G. Hesketh⁸¹, N.P. Hessey^{163a}, J.W. Hetherly⁴³, S. Higashino⁶⁹, E. Higón-Rodríguez¹⁷⁰, K. Hildebrand³³, E. Hill¹⁷², J.C. Hill³⁰, K.K. Hill²⁷, K.H. Hiller⁴⁵, S.J. Hillier¹⁹, M. Hils⁴⁷, I. Hinchliffe¹⁶, M. Hirose¹²⁰, D. Hirschbuehl¹⁷⁷, B. Hiti⁷⁸, O. Hladik¹²⁹, D.R. Hlaluku^{147c}, X. Hoad⁴⁹, J. Hobbs¹⁵⁰, N. Hod^{163a}, M.C. Hodgkinson¹⁴¹, A. Hoecker³², M.R. Hoferkamp¹⁰⁷, F. Hoenic¹⁰², D. Hohn²³, D. Hohov¹¹⁹, T.R. Holmes³³, M. Holzbock¹⁰², M. Homann⁴⁶, S. Honda¹⁶⁴, T. Honda⁶⁹, T.M. Hong¹²⁷, B.H. Hooberman¹⁶⁹, W.H. Hopkins¹¹⁸, Y. Horii¹⁰⁵, P. Horn⁴⁷, A.J. Horton¹⁴⁴, L.A. Horyn³³, J.-Y. Hostachy⁵⁷, A. Hostiuc¹⁴⁰, S. Hou¹⁵³, A. Hoummada^{137a}, J. Howarth⁸⁷, J. Hoya⁷⁴, M. Hrabovsky¹¹⁷, J. Hrdinka³², I. Hristova¹⁷, J. Hrivnac¹¹⁹, T. Hryn'ova⁵, A. Hrynevich⁹⁶, P.J. Hsu⁶³, S.-C. Hsu¹⁴⁰, Q. Hu²⁷, S. Hu^{36c}, Y. Huang^{35a}, Z. Hubacek¹³⁰, F. Hubaut⁸⁸, M. Huebner²³, F. Huegging²³, T.B. Huffman¹²², E.W. Hughes³⁸, M. Huhtinen³², R.F.H. Hunter³¹, P. Huo¹⁵⁰, A.M. Hupe³¹, N. Huseynov^{68,b}, J. Huston⁹³, J. Huth⁵⁹, R. Hyneman⁹², G. Iacobucci⁵², G. Iakovidis²⁷, I. Ibragimov¹⁴³, L. Iconomidou-Fayard¹¹⁹, Z. Idrissi^{137e}, P. Iengo³², R. Ignazzi³⁹, O. Igonkina^{109,aa}, R. Iguchi¹⁵⁷, T. Iizawa¹⁷⁴, Y. Ikegami⁶⁹, M. Ikeno⁶⁹, D. Iliadis¹⁵⁶, N. Ilic¹⁴⁵, F. Iltzsche⁴⁷, G. Introzzi^{123a,123b}, M. Iodice^{136a}, K. Iordanidou³⁸, V. Ippolito^{134a,134b}, M.F. Isacson¹⁶⁸, N. Ishijima¹²⁰, M. Ishino¹⁵⁷, M. Ishitsuka¹⁵⁹, C. Issever¹²², S. Istin^{20a,ba}, F. Ito¹⁶⁴, J.M. Iturbe Ponce^{62a}, R. Iuppa^{162a,162b}, A. Ivina¹⁷⁵, H. Iwasaki⁶⁹, J.M. Izen⁴⁴, V. Izzo^{106a}, S. Jabbar³, P. Jacka¹²⁹, P. Jackson¹, R.M. Jacobs²³, V. Jain², G. Jäkel¹⁷⁷, K.B. Jakobi⁸⁶, K. Jakobs⁵¹, S. Jakobsen⁶⁵, T. Jakoubek¹²⁹, D.O. Jamin¹¹⁶, D.K. Jana⁸², R. Jansky⁵², J. Janssen²³, M. Janus⁵⁸, P.A. Janus^{41a}, G. Jarlskog⁸⁴, N. Javadov^{68,b}, T. Javůrek⁵¹, M. Javurkova⁵¹, F. Jeanneau¹³⁸, L. Jeanty¹⁶, J. Jejelava^{54a,ab}, A. Jelinskas¹⁷³, P. Jenni^{51,ac}, J. Jeong⁴⁵, C. Jeske¹⁷³, S. Jézéquel⁵, H. Ji¹⁷⁶, J. Jia¹⁵⁰, H. Jiang⁶⁷, Y. Jiang^{36a}, Z. Jiang¹⁴⁵, S. Jiggins⁵¹, F.A. Jimenez Morales³⁷, J. Jimenez Pena¹⁷⁰, S. Jin^{35b}, A. Jinaru^{28b}, O. Jinnouchi¹⁵⁹, H. Jivan^{147c}, P. Johansson¹⁴¹, K.A. Johns⁷, C.A. Johnson⁶⁴, W.J. Johnson¹⁴⁰, K. Jon-And^{148a,148b}, R.W.L. Jones⁷⁵, S.D. Jones¹⁵¹, S. Jones⁷, T.J. Jones⁷⁷, J. Jongmanns^{60a}, P.M. Jorge^{128a,128b}, J. Jovicevic^{163a}, X. Ju¹⁷⁶, J.J. Junggeburth¹⁰³, A. Juste Rozas^{13,v}, A. Kaczmarska⁴², M. Kado¹¹⁹, H. Kagan¹¹³, M. Kagan¹⁴⁵, T. Kaji¹⁷⁴, E. Kajomovitz¹⁵⁴, C.W. Kalderon⁸⁴, A. Kaluza⁸⁶, S. Kama⁴³, A. Kamenshchikov¹³², L. Kanjir⁷⁸, Y. Kano¹⁵⁷, V.A. Kantserov¹⁰⁰, J. Kanzaki⁶⁹, B. Kaplan¹¹², L.S. Kaplan¹⁷⁶, D. Kar^{147c}, M.J. Kareem^{163b}, E. Karentzos¹⁰, S.N. Karpov⁶⁸, Z.M. Karpova⁶⁸, V. Kartvelishvili⁷⁵, A.N. Karyukhin¹³², K. Kasahara¹⁶⁴, L. Kashif¹⁷⁶, R.D. Kass¹¹³, A. Kastanas¹⁴⁹, Y. Kataoka¹⁵⁷, C. Kato¹⁵⁷, J. Katzy⁴⁵, K. Kawade⁷⁰, K. Kawagoe⁷³, T. Kawamoto¹⁵⁷, G. Kawamura⁵⁸, E.F. Kay⁷⁷, V.F. Kazanin^{111,c}, R. Keeler¹⁷², R. Kehoe⁴³, J.S. Keller³¹, E. Kellermann⁸⁴, J.J. Kempster¹⁹, J. Kendrick¹⁹, O. Kepka¹²⁹, B.P. Kerševan⁷⁸, S. Kersten¹⁷⁷, R.A. Keyes⁹⁰, M. Khader¹⁶⁹, F. Khalil-zada¹², A. Khanov¹¹⁶, A.G. Kharlamov^{111,c}, T. Kharlamova^{111,c}, A. Khodinov¹⁶⁰, T.J. Khoo⁵², E. Khramov⁶⁸, J. Khubua^{54b,ad}, S. Kido⁷⁰, M. Kiehn⁵², C.R. Kilby⁸⁰, S.H. Kim¹⁶⁴, Y.K. Kim³³, N. Kimura^{167a,167c}, O.M. Kind¹⁷, B.T. King⁷⁷, D. Kirchmeier⁴⁷, J. Kirk¹³³, A.E. Kiryunin¹⁰³, T. Kishimoto¹⁵⁷, D. Kisiielewska^{41a}, V. Kitali⁴⁵, O. Kivernyk⁵, E. Kladiva^{146b,*}, T. Klapdor-Kleingrothaus⁵¹, M.H. Klein⁹², M. Klein⁷⁷, U. Klein⁷⁷, K. Kleinknecht⁸⁶, P. Klimek¹¹⁰, A. Klimentov²⁷, R. Klingenberg^{46,*}, T. Klingl²³, T. Klioutchnikova³², F.F. Klitzner¹⁰², E.-E. Kluge^{60a}, P. Kluit¹⁰⁹, S. Kluth¹⁰³, E. Kneringer⁶⁵,

E.B.F.G. Knoops⁸⁸, A. Knue⁵¹, A. Kobayashi¹⁵⁷, D. Kobayashi⁷³, T. Kobayashi¹⁵⁷, M. Kobel⁴⁷, M. Kocian¹⁴⁵, P. Kodys¹³¹, T. Koffas³¹, E. Koffeman¹⁰⁹, N.M. Köhler¹⁰³, T. Koi¹⁴⁵, M. Kolb^{60b}, I. Koletsou⁵, T. Kondo⁶⁹, N. Kondrashova^{36c}, K. Köneke⁵¹, A.C. König¹⁰⁸, T. Kono⁶⁹, R. Konoplich^{112,ae}, N. Konstantinidis⁸¹, B. Konya⁸⁴, R. Kopeliansky⁶⁴, S. Koperny^{41a}, K. Korcyl⁴², K. Kordas¹⁵⁶, A. Korn⁸¹, I. Korolkov¹³, E.V. Korolkova¹⁴¹, O. Kortner¹⁰³, S. Kortner¹⁰³, T. Kosek¹³¹, V.V. Kostyukhin²³, A. Kotwal⁴⁸, A. Koulouris¹⁰, A. Kourkoumeli-Charalampidi^{123a,123b}, C. Kourkoumelis⁹, E. Kourlitis¹⁴¹, V. Kouskoura²⁷, A.B. Kowalewska⁴², R. Kowalewski¹⁷², T.Z. Kowalski^{41a}, C. Kozakai¹⁵⁷, W. Kozanecki¹³⁸, A.S. Kozhin¹³², V.A. Kramarenko¹⁰¹, G. Kramberger⁷⁸, D. Krasnoperstev¹⁰⁰, M.W. Krasny⁸³, A. Krasznahorkay³², D. Krauss¹⁰³, J.A. Kremer^{41a}, J. Kretschmar⁷⁷, P. Krieger¹⁶¹, K. Krizka¹⁶, K. Kroeninger⁴⁶, H. Kroha¹⁰³, J. Kroll¹²⁹, J. Kroll¹²⁴, J. Krstic¹⁴, U. Kruchonak⁶⁸, H. Krüger²³, N. Krumnack⁶⁷, M.C. Kruse⁴⁸, T. Kubota⁹¹, S. Kudah^{4b}, J.T. Kuechler¹⁷⁷, S. Kuehn³², A. Kugel^{60a}, F. Kuger¹⁷⁸, T. Kuhl⁴⁵, V. Kukhtin⁶⁸, R. Kukla⁸⁸, Y. Kulchitsky⁹⁵, S. Kuleshov^{34b}, Y.P. Kulinich¹⁶⁹, M. Kuna⁵⁷, T. Kunigo⁷¹, A. Kupco¹²⁹, T. Kupfer⁴⁶, O. Kuprash¹⁵⁵, H. Kurashige⁷⁰, L.L. Kurchaninov^{163a}, Y.A. Kurochkin⁹⁵, M.G. Kurth^{35a,35d}, E.S. Kuwertz¹⁷², M. Kuze¹⁵⁹, J. Kvita¹¹⁷, T. Kwan¹⁷², A. La Rosa¹⁰³, J.L. La Rosa Navarro^{26d}, L. La Rotonda^{40a,40b}, F. La Ruffa^{40a,40b}, C. Lacasta¹⁷⁰, F. Lacava^{134a,134b}, J. Lacey⁴⁵, D.P.J. Lack⁸⁷, H. Lacker¹⁷, D. Lacour⁸³, E. Ladygin⁶⁸, R. Lafaye⁵, B. Laforge⁸³, T. Lagouri^{147c}, S. Lai⁵⁸, S. Lammers⁶⁴, W. Lampl⁷, E. Lançon²⁷, U. Landgraf⁵¹, M.P.J. Landon⁷⁹, M.C. Lanfermann⁵², V.S. Lang⁴⁵, J.C. Lange¹³, R.J. Langenberg³², A.J. Lankford¹⁶⁶, F. Lanni²⁷, K. Lantsch²³, A. Lanza^{123a}, A. Lapertosa^{53a,53b}, S. Laplace⁸³, J.F. Laporte¹³⁸, T. Lari^{94a}, F. Lasagni Manghi^{22a,22b}, M. Lassnig³², T.S. Lau^{62a}, A. Laudrain¹¹⁹, A.T. Law¹³⁹, P. Laycock⁷⁷, M. Lazzaroni^{94a,94b}, B. Le⁹¹, O. Le Dortz⁸³, E. Le Guirriec⁸⁸, E.P. Le Quilleuc¹³⁸, M. LeBlanc⁷, T. LeCompte⁶, F. Ledroit-Guillon⁵⁷, C.A. Lee²⁷, G.R. Lee^{34a}, S.C. Lee¹⁵³, L. Lee⁵⁹, B. Lefebvre⁹⁰, M. Lefebvre¹⁷², F. Legger¹⁰², C. Leggett¹⁶, G. Lehmann Miotto³², W.A. Leight⁴⁵, A. Leisos^{156,af}, M.A.L. Leite^{26d}, R. Leitner¹³¹, D. Lellouch¹⁷⁵, B. Lemmer⁵⁸, K.J.C. Leney⁸¹, T. Lenz²³, B. Lenzi³², R. Leone⁷, S. Leone^{126a}, C. Leonidopoulos⁴⁹, G. Lerner¹⁵¹, C. Leroy⁹⁷, R. Les¹⁶¹, A.A.J. Lesage¹³⁸, C.G. Lester³⁰, M. Levchenko¹²⁵, J. Levêque⁵, D. Levin⁹², L.J. Levinson¹⁷⁵, D. Lewis⁷⁹, B. Li⁹², C.-Q. Li^{36a}, H. Li^{36b}, L. Li^{36c}, Q. Li^{35a,35d}, Q. Li^{36a}, S. Li^{36c,36d}, X. Li^{36c}, Y. Li¹⁴³, Z. Liang^{35a}, B. Liberti^{135a}, A. Liblong¹⁶¹, K. Lie^{62c}, S. Liem¹⁰⁹, A. Limosani¹⁵², C.Y. Lin³⁰, K. Lin⁹³, S.C. Lin¹⁸², T.H. Lin⁸⁶, R.A. Linck⁶⁴, B.E. Lindquist¹⁵⁰, A.L. Lioni⁵², E. Lipeles¹²⁴, A. Lipniacka¹⁵, M. Lisovsky^{60b}, T.M. Liss^{169,ag}, A. Lister¹⁷¹, A.M. Litke¹³⁹, J.D. Little⁸, B.L. Liu⁶, B. Liu⁶⁷, H. Liu⁹², H. Liu²⁷, J.K.K. Liu¹²², J.B. Liu^{36a}, K. Liu⁸³, M. Liu^{36a}, P. Liu¹⁶, Y.L. Liu^{36a}, Y. Liu^{36a}, M. Livan^{123a,123b}, A. Lleres⁵⁷, J. Llorente Merino^{35a}, S.L. Lloyd⁷⁹, C.Y. Lo^{62b}, F. Lo Sterzo⁴³, E.M. Lobodzinska⁴⁵, P. Loch⁷, F.K. Loebinger⁸⁷, A. Loesle⁵¹, K.M. Loew²⁵, T. Lohse¹⁷, K. Lohwasser¹⁴¹, M. Lokajicek¹²⁹, B.A. Long²⁴, J.D. Long¹⁶⁹, R.E. Long⁷⁵, L. Longo^{76a,76b}, K.A. Looper¹¹³, J.A. Lopez^{34b}, I. Lopez Paz¹³, A. Lopez Solis⁸³, J. Lorenz¹⁰², N. Lorenzo Martinez⁵, M. Losada²¹, P.J. Lösel¹⁰², X. Lou^{35a}, X. Lou⁴⁵, A. Lounis¹¹⁹, J. Love⁶, P.A. Love⁷⁵, J.J. Lozano Bahilo¹⁷⁰, H. Lu^{62a}, N. Lu⁹², Y.J. Lu⁶³, H.J. Lubatti¹⁴⁰, C. Luci^{134a,134b}, A. Lucotte⁵⁷, C. Luedtke⁵¹, F. Luehring⁶⁴, I. Luise⁸³, W. Lukas⁶⁵, L. Luminari^{134a}, B. Lund-Jensen¹⁴⁹, M.S. Lutz⁸⁹, P.M. Luzi⁸³, D. Lynn²⁷, R. Lysak¹²⁹, E. Lytken⁸⁴, F. Lyu^{35a}, V. Lyubushkin⁶⁸, H. Ma²⁷, L.L. Ma^{36b}, Y. Ma^{36b}, G. Maccarrone⁵⁰, A. Macchiolo¹⁰³, C.M. Macdonald¹⁴¹, B. Maček⁷⁸, J. Machado Miguens^{124,128b}, D. Madaffari¹⁷⁰, R. Madar³⁷, W.F. Mader⁴⁷, A. Madsen⁴⁵, N. Madysa⁴⁷, J. Maeda⁷⁰, S. Maeland¹⁵, T. Maeno²⁷, A.S. Maevskiy¹⁰¹, V. Magerl⁵¹, C. Maidantchik^{26a}, T. Maier¹⁰², A. Maio^{128a,bb}, O. Majersky^{146a}, S. Majewski¹¹⁸, Y. Makida⁶⁹, N. Makovec¹¹⁹, B. Malaescu⁸³, Pa. Malecki⁴², V.P. Maleev¹²⁵, F. Malek⁵⁷, U. Mallik⁶⁶, D. Malon⁶, C. Malone³⁰, S. Maltezos¹⁰, S. Malyukov³², J. Mamuzic¹⁷⁰, G. Mancini⁵⁰, I. Mandić⁷⁸, J. Maneira^{128a,128b}, L. Manhaes de Andrade Filho^{26b}, J. Manjarres Ramos⁴⁷, K.H. Mankinen⁸⁴, A. Mann¹⁰², A. Manousos⁶⁵, B. Mansoulie¹³⁸, J.D. Mansour^{35a}, M. Mantoani⁵⁸, S. Manzoni^{94a,94b}, G. Marceca²⁹, L. March⁵², L. Marchese¹²², G. Marchiori⁸³, M. Marcisovsky¹²⁹, C.A. Marin Tobon³², M. Marjanovic³⁷, D.E. Marley⁹², F. Marroquim^{26a}, Z. Marshall¹⁶, M.U.F. Martensson¹⁶⁸, S. Marti-Garcia¹⁷⁰, C.B. Martin¹¹³, T.A. Martin¹⁷³, V.J. Martin⁴⁹, B. Martin dit Latour¹⁵, M. Martinez^{13,v}, V.I. Martinez Outschoorn⁸⁹, S. Martin-Haugh¹³³, V.S. Martoiu^{28b}, A.C. Martyniuk⁸¹, A. Marzin³², L. Masetti⁸⁶, T. Mashimo¹⁵⁷, R. Mashinistov⁹⁸, J. Masik⁸⁷, A.L. Maslennikov^{111,c}, L.H. Mason⁹¹, L. Massa^{135a,135b}, P. Mastrandrea⁵, A. Mastroberardino^{40a,40b}, T. Masubuchi¹⁵⁷, P. Mättig¹⁷⁷, J. Maurer^{28b}, S.J. Maxfield⁷⁷, D.A. Maximov^{111,c}, R. Mazini¹⁵³, I. Maznas¹⁵⁶, S.M. Mazza¹³⁹,

N.C. Mc Fadden¹⁰⁷, G. Mc Goldrick¹⁶¹, S.P. Mc Kee⁹², A. McCarn⁹², T.G. McCarthy¹⁰³, L.I. McClymont⁸¹, E.F. McDonald⁹¹, J.A. Mcfayden³², G. Mchedlidze⁵⁸, M.A. McKay⁴³, K.D. McLean¹⁷², S.J. McMahon¹³³, P.C. McNamara⁹¹, C.J. McNicol¹⁷³, R.A. McPherson^{172,n}, J.E. Mdhului^{147c}, Z.A. Meadows⁸⁹, S. Meehan¹⁴⁰, T. Megy⁵¹, S. Mehlhase¹⁰², A. Mehta⁷⁷, T. Meideck⁵⁷, K. Meier^{60a}, B. Meirose⁴⁴, D. Melini^{170,ah}, B.R. Mellado Garcia^{147c}, J.D. Mellenthin⁵⁸, M. Melo^{146a}, F. Meloni¹⁸, A. Melzer²³, S.B. Menary⁸⁷, L. Meng⁷⁷, X.T. Meng⁹², A. Mengarelli^{22a,22b}, S. Menke¹⁰³, E. Meoni^{40a,40b}, S. Mergelmeyer¹⁷, C. Merlassino¹⁸, P. Mermod⁵², L. Merola^{106a,106b}, C. Meroni^{94a}, F.S. Merritt³³, A. Messina^{134a,134b}, J. Metcalfe⁶, A.S. Mete¹⁶⁶, C. Meyer¹²⁴, J-P. Meyer¹³⁸, J. Meyer¹⁵⁴, H. Meyer Zu Theenhausen^{60a}, F. Miano¹⁵¹, R.P. Middleton¹³³, L. Mijović⁴⁹, G. Mikenberg¹⁷⁵, M. Mikestikova¹²⁹, M. Mikuž⁷⁸, M. Milesi⁹¹, A. Milic¹⁶¹, D.A. Millar⁷⁹, D.W. Miller³³, A. Milov¹⁷⁵, D.A. Milstead^{148a,148b}, A.A. Minaenko¹³², I.A. Minashvili^{54b}, A.I. Mincer¹¹², B. Mindur^{41a}, M. Mineev⁶⁸, Y. Minegishi¹⁵⁷, Y. Ming¹⁷⁶, L.M. Mir¹³, A. Mirto^{76a,76b}, K.P. Mistry¹²⁴, T. Mitani¹⁷⁴, J. Mitrevski¹⁰², V.A. Mitsou¹⁷⁰, A. Miucci¹⁸, P.S. Miyagawa¹⁴¹, A. Mizukami⁶⁹, J.U. Mjörnmark⁸⁴, T. Mkrtchyan¹⁸⁰, M. Mlynarikova¹³¹, T. Moa^{148a,148b}, K. Mochizuki⁹⁷, P. Mogg⁵¹, S. Mohapatra³⁸, S. Molander^{148a,148b}, R. Moles-Valls²³, M.C. Mondragon⁹³, K. Mönig⁴⁵, J. Monk³⁹, E. Monnier⁸⁸, A. Montalbano¹⁴⁴, J. Montejo Berlingen³², F. Monticelli⁷⁴, S. Monzani^{94a}, R.W. Moore³, N. Morange¹¹⁹, D. Moreno²¹, M. Moreno Llacer³², P. Morettini^{53a}, M. Morgenstern¹⁰⁹, S. Morgenstern³², D. Mori¹⁴⁴, T. Mori¹⁵⁷, M. Morii⁵⁹, M. Morinaga¹⁷⁴, V. Morisbak¹²¹, A.K. Morley³², G. Mornacchi³², J.D. Morris⁷⁹, L. Morvaj¹⁵⁰, P. Moschovakos¹⁰, M. Mosidze^{54b}, H.J. Moss¹⁴¹, J. Moss^{145,ai}, K. Motohashi¹⁵⁹, R. Mount¹⁴⁵, E. Mountricha²⁷, E.J.W. Moyse⁸⁹, S. Muanza⁸⁸, F. Mueller¹⁰³, J. Mueller¹²⁷, R.S.P. Mueller¹⁰², D. Muenstermann⁷⁵, P. Mullen⁵⁶, G.A. Mullier¹⁸, F.J. Munoz Sanchez⁸⁷, P. Murin^{146b}, W.J. Murray^{173,133}, A. Murrone^{94a,94b}, M. Muškinja⁷⁸, C. Mwewa^{147a}, A.G. Myagkov^{132,aj}, J. Myers¹¹⁸, M. Myska¹³⁰, B.P. Nachman¹⁶, O. Nackenhorst⁴⁶, K. Nagai¹²², R. Nagai^{69,ak}, K. Nagano⁶⁹, Y. Nagasaka⁶¹, K. Nagata¹⁶⁴, M. Nagel⁵¹, E. Nagy⁸⁸, A.M. Nairz³², Y. Nakahama¹⁰⁵, K. Nakamura⁶⁹, T. Nakamura¹⁵⁷, I. Nakano¹¹⁴, F. Napolitano^{60a}, R.F. Naranjo Garcia⁴⁵, R. Narayan¹¹, D.I. Narrias Villar^{60a}, I. Naryshkin¹²⁵, T. Naumann⁴⁵, G. Navarro²¹, R. Nayyar⁷, H.A. Neal⁹², P.Yu. Nechaeva⁹⁸, T.J. Neep¹³⁸, A. Negri^{123a,123b}, M. Negrini^{22a}, S. Nektarijevic¹⁰⁸, C. Nellist⁵⁸, M.E. Nelson¹²², S. Nemecek¹²⁹, P. Nemethy¹¹², M. Nessi^{32,al}, M.S. Neubauer¹⁶⁹, M. Neumann¹⁷⁷, P.R. Newman¹⁹, T.Y. Ng^{62c}, Y.S. Ng¹⁷, H.D.N. Nguyen⁸⁸, T. Nguyen Manh⁹⁷, E. Nibigira³⁷, R.B. Nickerson¹²², R. Nicolaidou¹³⁸, J. Nielsen¹³⁹, N. Nikiforou¹¹, V. Nikolaenko^{132,aj}, I. Nikolic-Audit⁸³, K. Nikolopoulos¹⁹, P. Nilsson²⁷, Y. Ninomiya⁶⁹, A. Nisati^{134a}, N. Nishu^{36c}, R. Nisius¹⁰³, I. Nitsche⁴⁶, T. Nitta¹⁷⁴, T. Nobe¹⁵⁷, Y. Noguchi⁷¹, M. Nomachi¹²⁰, I. Nomidis³¹, M.A. Nomura²⁷, T. Nooney⁷⁹, M. Nordberg³², N. Norjoharuddeen¹²², T. Novak⁷⁸, O. Novgorodova⁴⁷, R. Novotny¹³⁰, M. Nozaki⁶⁹, L. Nozka¹¹⁷, K. Ntekas¹⁶⁶, E. Nurse⁸¹, F. Nuti⁹¹, K. O'Connor²⁵, D.C. O'Neil¹⁴⁴, A.A. O'Rourke⁴⁵, V. O'Shea⁵⁶, F.G. Oakham^{31,d}, H. Oberlack¹⁰³, T. Obermann²³, J. Ocariz⁸³, A. Ochi⁷⁰, I. Ochoa³⁸, J.P. Ochoa-Ricoux^{34a}, S. Oda⁷³, S. Odaka⁶⁹, A. Oh⁸⁷, S.H. Oh⁴⁸, C.C. Ohm¹⁴⁹, H. Oide^{53a,53b}, H. Okawa¹⁶⁴, Y. Okazaki⁷¹, Y. Okumura¹⁵⁷, T. Okuyama⁶⁹, A. Olariu^{28b}, L.F. Oleiro Seabra^{128a}, S.A. Olivares Pino^{34a}, D. Oliveira Damazio²⁷, J.L. Oliver¹, M.J.R. Olsson³³, A. Olszewski⁴², J. Olszowska⁴², A. Onofre^{128a,128e}, K. Onogi¹⁰⁵, P.U.E. Onyisi^{11,am}, H. Oppen¹²¹, M.J. Oreglia³³, Y. Oren¹⁵⁵, D. Orestano^{136a,136b}, E.C. Orgill⁸⁷, N. Orlando^{62b}, R.S. Orr¹⁶¹, B. Osculati^{53a,53b,*}, R. Ospanov^{36a}, G. Otero y Garzon²⁹, H. Otono⁷³, M. Ouchrif^{137d}, F. Ould-Saada¹²¹, A. Ouraou¹³⁸, Q. Ouyang^{35a}, M. Owen⁵⁶, R.E. Owen¹⁹, V.E. Ozcan^{20a}, N. Ozturk⁸, H.A. Pacey³⁰, K. Pachal¹⁴⁴, A. Pacheco Pages¹³, L. Pacheco Rodriguez¹³⁸, C. Padilla Aranda¹³, S. Pagan Griso¹⁶, M. Paganini¹⁷⁹, F. Paige²⁷, G. Palacino⁶⁴, S. Palazzo^{40a,40b}, S. Palestini³², M. Palka^{41b}, D. Pallin³⁷, I. Panagoulas¹⁰, C.E. Pandini⁵², J.G. Panduro Vazquez⁸⁰, P. Pani³², L. Paolozzi⁵², Th.D. Papadopoulou¹⁰, K. Papageorgiou^{9,s}, A. Paramonov⁶, D. Paredes Hernandez^{62b}, B. Parida^{36c}, A.J. Parker⁷⁵, M.A. Parker³⁰, K.A. Parker⁴⁵, F. Parodi^{53a,53b}, J.A. Parsons³⁸, U. Parzefall⁵¹, V.R. Pascuzzi¹⁶¹, J.M.P. Pasner¹³⁹, E. Pasqualucci^{134a}, S. Passaggio^{53a}, Fr. Pastore⁸⁰, P. Pasuwan^{148a,148b}, S. Patariaia⁸⁶, J.R. Pater⁸⁷, A. Pathak^{176,e}, T. Pauly³², B. Pearson¹⁰³, M. Pedersen¹²¹, S. Pedraza Lopez¹⁷⁰, R. Pedro^{128a,128b}, S.V. Peleganchuk^{111,c}, O. Penc¹²⁹, C. Peng^{35a,35d}, H. Peng^{36a}, B.S. Peralva^{26b}, M.M. Perego¹³⁸, A.P. Pereira Peixoto^{128a}, D.V. Perepelitsa²⁷, F. Peri¹⁷, L. Perini^{94a,94b}, H. Pernegger³², S. Perrella^{106a,106b}, V.D. Peshekhonov^{68,*}, K. Peters⁴⁵, R.F.Y. Peters⁸⁷, B.A. Petersen³², T.C. Petersen³⁹, E. Petit⁵⁷, A. Petridis¹, C. Petridou¹⁵⁶, P. Petroff¹¹⁹, E. Petrolo^{134a}, M. Petrov¹²², F. Petrucci^{136a,136b},

N.E. Pettersson⁸⁹, A. Peyaud¹³⁸, R. Pezoa^{34b}, T. Pham⁹¹, F.H. Phillips⁹³, P.W. Phillips¹³³,
 G. Piacquadio¹⁵⁰, E. Pianori¹⁶, A. Picazio⁸⁹, M.A. Pickering¹²², R. Piegai²⁹, J.E. Pilcher³³,
 A.D. Pilkington⁸⁷, M. Pinamonti^{135a,135b}, J.L. Pinfold³, M. Pitt¹⁷⁵, M.-A. Pleier²⁷, V. Pleskot¹³¹,
 E. Plotnikova⁶⁸, D. Pluth⁶⁷, P. Podberezko¹¹¹, R. Poettgen⁸⁴, R. Poggi^{123a,123b}, L. Poggioli¹¹⁹,
 I. Pogrebnyak⁹³, D. Pohl²³, I. Pokharel⁵⁸, G. Polesello^{123a}, A. Poley⁴⁵, A. Policicchio^{40a,40b}, R. Polifka³²,
 A. Polini^{22a}, C.S. Pollard⁴⁵, V. Polychronakos²⁷, D. Ponomarenko¹⁰⁰, L. Pontecorvo^{134a},
 G.A. Popeneciu^{28d}, D.M. Portillo Quintero⁸³, S. Pospisil¹³⁰, K. Potamianos⁴⁵, I.N. Potrap⁶⁸, C.J. Potter³⁰,
 H. Potti¹¹, T. Poulsen⁸⁴, J. Poveda³², T.D. Powell¹⁴¹, M.E. Pozo Astigarraga³², P. Pralavorio⁸⁸, S. Prell⁶⁷,
 D. Price⁸⁷, M. Primavera^{76a}, S. Prince⁹⁰, N. Proklova¹⁰⁰, K. Prokofiev^{62c}, F. Prokoshin^{34b},
 S. Protopopescu²⁷, J. Proudfoot⁶, M. Przybycien^{41a}, A. Puri¹⁶⁹, P. Puzo¹¹⁹, J. Qian⁹², Y. Qin⁸⁷,
 A. Quadt⁵⁸, M. Queitsch-Maitland⁴⁵, A. Qureshi¹, P. Rados⁹¹, F. Ragusa^{94a,94b}, G. Rahal¹⁸¹, J.A. Raine⁸⁷,
 S. Rajagopalan²⁷, T. Rashid¹¹⁹, S. Raspopov⁵, M.G. Ratti^{94a,94b}, D.M. Rauch⁴⁵, F. Rauscher¹⁰², S. Rave⁸⁶,
 B. Ravina¹⁴¹, I. Ravinovich¹⁷⁵, J.H. Rawling⁸⁷, M. Raymond³², A.L. Read¹²¹, N.P. Readoff⁵⁷,
 M. Reale^{76a,76b}, D.M. Rebuzzi^{123a,123b}, A. Redelbach¹⁷⁸, G. Redlinger²⁷, R. Reece¹³⁹, R.G. Reed^{147c},
 K. Reeves⁴⁴, L. Rehnisch¹⁷, J. Reichert¹²⁴, A. Reiss⁸⁶, C. Rembser³², H. Ren^{35a,35d}, M. Rescigno^{134a},
 S. Resconi^{94a}, E.D. Resseguie¹²⁴, S. Rettie¹⁷¹, E. Reynolds¹⁹, O.L. Rezanova^{111.c}, P. Reznicek¹³¹,
 R. Richter¹⁰³, S. Richter⁸¹, E. Richter-Was^{41b}, O. Ricken²³, M. Ridel⁸³, P. Rieck¹⁰³, C.J. Riegel¹⁷⁷,
 O. Rifki⁴⁵, M. Rijssenbeek¹⁵⁰, A. Rimoldi^{123a,123b}, M. Rimoldi¹⁸, L. Rinaldi^{22a}, G. Ripellino¹⁴⁹,
 B. Ristić⁷⁵, E. Ritsch³², I. Riu¹³, J.C. Rivera Vergara^{34a}, F. Rizatdinova¹¹⁶, E. Rizvi⁷⁹, C. Rizzi¹³,
 R.T. Roberts⁸⁷, S.H. Robertson^{90,n}, A. Robichaud-Veronneau⁹⁰, D. Robinson³⁰, J.E.M. Robinson⁴⁵,
 A. Robson⁵⁶, E. Rocco⁸⁶, C. Roda^{126a,126b}, Y. Rodina^{88.an}, S. Rodriguez Bosca¹⁷⁰, A. Rodriguez Perez¹³,
 D. Rodriguez Rodriguez¹⁷⁰, A.M. Rodríguez Vera^{163b}, S. Roe³², C.S. Rogan⁵⁹, O. Röhne¹²¹, R. Röhrig¹⁰³,
 C.P.A. Roland⁶⁴, J. Roloff⁵⁹, A. Romaniouk¹⁰⁰, M. Romano^{22a,22b}, N. Rompotis⁷⁷, M. Ronzani¹¹²,
 L. Roos⁸³, S. Rosati^{134a}, K. Rosbach⁵¹, P. Rose¹³⁹, N.-A. Rosien⁵⁸, E. Rossi^{106a,106b}, L.P. Rossi^{53a},
 L. Rossini^{94a,94b}, J.H.N. Rosten³⁰, R. Rosten¹⁴⁰, M. Rotaru^{28b}, J. Rothberg¹⁴⁰, D. Rousseau¹¹⁹, D. Roy^{147c},
 A. Rozanov⁸⁸, Y. Rozen¹⁵⁴, X. Ruan^{147c}, F. Rubbo¹⁴⁵, F. Rühr⁵¹, A. Ruiz-Martinez³¹, Z. Rurikova⁵¹,
 N.A. Rusakovich⁶⁸, H.L. Russell⁹⁰, J.P. Rutherford⁷, N. Ruthmann³², E.M. Rüttinger⁴⁵, Y.F. Ryabov¹²⁵,
 M. Rybar¹⁶⁹, G. Rybkin¹¹⁹, S. Ryu⁶, A. Ryzhov¹³², G.F. Rzehorz⁵⁸, A.F. Saavedra¹⁵², P. Sabatini⁵⁸,
 G. Sabato¹⁰⁹, S. Sacerdoti¹¹⁹, H.F.-W. Sadrozinski¹³⁹, R. Sadykov⁶⁸, F. Safai Tehrani^{134a}, P. Saha¹¹⁰,
 M. Sahinsoy^{60a}, A. Sahu¹⁷⁷, M. Saimpert⁴⁵, M. Saito¹⁵⁷, T. Saito¹⁵⁷, H. Sakamoto¹⁵⁷, A. Sakharov¹¹²,
 D. Salamani⁵², G. Salamanna^{136a,136b}, J.E. Salazar Loyola^{34b}, D. Salek¹⁰⁹, P.H. Sales De Bruin¹⁶⁸,
 D. Saliagic¹⁰³, A. Salnikov¹⁴⁵, J. Salt¹⁷⁰, D. Salvatore^{40a,40b}, F. Salvatore¹⁵¹, A. Salvucci^{62a,62b,62c},
 A. Salzburger³², D. Sammel⁵¹, D. Sampsonidis¹⁵⁶, D. Sampsonidou¹⁵⁶, J. Sánchez¹⁷⁰,
 A. Sanchez Pineda^{167a,167c}, H. Sandaker¹²¹, C.O. Sander⁴⁵, M. Sandhoff¹⁷⁷, C. Sandoval²¹,
 D.P.C. Sankey¹³³, M. Sannino^{53a,53b}, Y. Sano¹⁰⁵, A. Sansoni⁵⁰, C. Santoni³⁷, H. Santos^{128a},
 I. Santoyo Castillo¹⁵¹, A. Saponov⁶⁸, J.G. Saraiva^{128a}, O. Sasaki⁶⁹, K. Sato¹⁶⁴, E. Sauvan⁵, P. Savard^{161.d},
 N. Savic¹⁰³, R. Sawada¹⁵⁷, C. Sawyer¹³³, L. Sawyer^{82.u}, C. Sbarra^{22a}, A. Sbrizzi^{22a,22b}, T. Scanlon⁸¹,
 D.A. Scannicchio¹⁶⁶, J. Schaarschmidt¹⁴⁰, P. Schacht¹⁰³, B.M. Schachtner¹⁰², D. Schaefer³³,
 L. Schaefer¹²⁴, J. Schaeffer⁸⁶, S. Schaepe³², U. Schäfer⁸⁶, A.C. Schaffer¹¹⁹, D. Schaile¹⁰²,
 R.D. Schamberger¹⁵⁰, N. Scharmberg⁸⁷, V.A. Schegelsky¹²⁵, D. Scheirich¹³¹, F. Schenck¹⁷,
 M. Schernau¹⁶⁶, C. Schiavi^{53a,53b}, S. Schier¹³⁹, L.K. Schildgen²³, Z.M. Schillaci²⁵, E.J. Schioppa³²,
 M. Schioppa^{40a,40b}, K.E. Schleicher⁵¹, S. Schlenker³², K.R. Schmidt-Sommerfeld¹⁰³, K. Schmieden³²,
 C. Schmitt⁸⁶, S. Schmitt⁴⁵, S. Schmitz⁸⁶, U. Schnoor⁵¹, L. Schoeffel¹³⁸, A. Schoening^{60b}, E. Schopf²³,
 M. Schott⁸⁶, J.F.P. Schouwenberg¹⁰⁸, J. Schovancova³², S. Schramm⁵², N. Schuh⁸⁶, A. Schulte⁸⁶,
 H.-C. Schultz-Coulon^{60a}, M. Schumacher⁵¹, B.A. Schumm¹³⁹, Ph. Schune¹³⁸, A. Schwartzman¹⁴⁵,
 T.A. Schwarz⁹², H. Schweiger⁸⁷, Ph. Schwemling¹³⁸, R. Schwienhorst⁹³, J. Schwindling¹³⁸,
 A. Sciandra²³, G. Sciolla²⁵, M. Scornajenghi^{40a,40b}, F. Scuri^{126a}, F. Scutti⁹¹, L.M. Scyboz¹⁰³, J. Searcy⁹²,
 C.D. Sebastiani^{134a,134b}, P. Seema²³, S.C. Seidel¹⁰⁷, A. Seiden¹³⁹, T. Seiss³³, J.M. Seixas^{26a},
 G. Sekhniaidze^{106a}, K. Sekhon⁹², S.J. Sekula⁴³, N. Semprini-Cesari^{22a,22b}, S. Sen⁴⁸, S. Senkin³⁷,
 C. Serfon¹²¹, L. Serin¹¹⁹, L. Serkin^{167a,167b}, M. Sessa^{136a,136b}, H. Severini¹¹⁵, T. Šfiligoj⁷⁸, F. Sforza¹⁶⁵,
 A. Sfyrla⁵², E. Shabalina⁵⁸, J.D. Shahinian¹³⁹, N.W. Shaikh^{148a,148b}, L.Y. Shan^{35a}, R. Shang¹⁶⁹,
 J.T. Shank²⁴, M. Shapiro¹⁶, A. Sharma¹²², A.S. Sharma¹, P.B. Shatalov⁹⁹, K. Shaw^{167a,167b}, S.M. Shaw⁸⁷,

A. Shcherbakova¹²⁵, C.Y. Shehu¹⁵¹, Y. Shen¹¹⁵, N. Sherafati³¹, A.D. Sherman²⁴, P. Sherwood⁸¹,
 L. Shi^{153,ao}, S. Shimizu⁷⁰, C.O. Shimmin¹⁷⁹, M. Shimojima¹⁰⁴, I.P.J. Shipsey¹²², S. Shirabe⁷³,
 M. Shiyakova^{68,ap}, J. Shlomi¹⁷⁵, A. Shmeleva⁹⁸, D. Shoaleh Saadi⁹⁷, M.J. Shochet³³, S. Shojaii⁹¹,
 D.R. Shope¹¹⁵, S. Shrestha¹¹³, E. Shulga¹⁰⁰, P. Sicho¹²⁹, A.M. Sickles¹⁶⁹, P.E. Sidebo¹⁴⁹,
 E. Sideras Haddad^{147c}, O. Sidiropoulou¹⁷⁸, A. Sidoti^{22a,22b}, F. Siegert⁴⁷, Dj. Sijacki¹⁴, J. Silva^{128a},
 M. Silva Jr.¹⁷⁶, S.B. Silverstein^{148a}, L. Simic⁶⁸, S. Simion¹¹⁹, E. Simioni⁸⁶, M. Simon⁸⁶, P. Sinervo¹⁶¹,
 N.B. Sinev¹¹⁸, M. Sioli^{22a,22b}, G. Siragusa¹⁷⁸, I. Siral⁹², S.Yu. Sivoklov¹⁰¹, J. Sjölin^{148a,148b},
 M.B. Skinner⁷⁵, P. Skubic¹¹⁵, M. Slater¹⁹, T. Slavicek¹³⁰, M. Slawinska⁴², K. Sliwa¹⁶⁵, R. Slovak¹³¹,
 V. Smakhtin¹⁷⁵, B.H. Smart⁵, J. Smiesko^{146a}, N. Smirnov¹⁰⁰, S.Yu. Smirnov¹⁰⁰, Y. Smirnov¹⁰⁰,
 L.N. Smirnova^{101,aq}, O. Smirnova⁸⁴, J.W. Smith⁵⁸, M.N.K. Smith³⁸, R.W. Smith³⁸, M. Smizanska⁷⁵,
 K. Smolek¹³⁰, A.A. Snesarev⁹⁸, I.M. Snyder¹¹⁸, S. Snyder²⁷, R. Sobie^{172,n}, A.M. Soffa¹⁶⁶, A. Soffer¹⁵⁵,
 A. Sogaard⁴⁹, D.A. Soh¹⁵³, G. Sokhrannyi⁷⁸, C.A. Solans Sanchez³², M. Solar¹³⁰, E.Yu. Soldatov¹⁰⁰,
 U. Soldevila¹⁷⁰, A.A. Solodkov¹³², A. Soloshenko⁶⁸, O.V. Solovyanov¹³², V. Solovyev¹²⁵, P. Sommer¹⁴¹,
 H. Son¹⁶⁵, W. Song¹³³, A. Sopczak¹³⁰, F. Sopkova^{146b}, D. Sosa^{60b}, C.L. Sotiropoulou^{126a,126b},
 S. Sottocornola^{123a,123b}, R. Soualah^{167a,167c}, A.M. Soukharev^{111,c}, D. South⁴⁵, B.C. Sowden⁸⁰,
 S. Spagnolo^{76a,76b}, M. Spalla¹⁰³, M. Spangenberg¹⁷³, F. Spanò⁸⁰, D. Sperlich¹⁷, F. Spettel¹⁰³,
 T.M. Spieker^{60a}, R. Spighi^{22a}, G. Spigo³², L.A. Spiller⁹¹, M. Spousta¹³¹, A. Stabile^{94a,94b}, R. Stamen^{60a},
 S. Stamm¹⁷, E. Stanecka⁴², R.W. Stanek⁶, C. Stanescu^{136a}, M.M. Stanitzki⁴⁵, B.S. Stapf¹⁰⁹, S. Stapnes¹²¹,
 E.A. Starchenko¹³², G.H. Stark³³, J. Stark⁵⁷, S.H. Stark³⁹, P. Staroba¹²⁹, P. Starovoitov^{60a}, S. Stärz³²,
 R. Staszewski⁴², M. Stegler⁴⁵, P. Steinberg²⁷, B. Stelzer¹⁴⁴, H.J. Stelzer³², O. Stelzer-Chilton^{163a},
 H. Stenzel⁵⁵, T.J. Stevenson⁷⁹, G.A. Stewart³², M.C. Stockton¹¹⁸, G. Stoica^{28b}, P. Stolte⁵⁸, S. Stonjek¹⁰³,
 A. Straessner⁴⁷, J. Strandberg¹⁴⁹, S. Strandberg^{148a,148b}, M. Strauss¹¹⁵, P. Strizenc^{146b}, R. Ströhmer¹⁷⁸,
 D.M. Strom¹¹⁸, R. Stroynowski⁴³, A. Strubig⁴⁹, S.A. Stucci²⁷, B. Stugu¹⁵, J. Stupak¹¹⁵, N.A. Styles⁴⁵,
 D. Su¹⁴⁵, J. Su¹²⁷, S. Suchek^{60a}, Y. Sugaya¹²⁰, M. Suk¹³⁰, V.V. Sulin⁹⁸, D.M.S. Sultan⁵², S. Sultansoy^{4c},
 T. Sumida⁷¹, S. Sun⁹², X. Sun³, K. Suruliz¹⁵¹, C.J.E. Suster¹⁵², M.R. Sutton¹⁵¹, S. Suzuki⁶⁹, M. Svatos¹²⁹,
 M. Swiatlowski³³, S.P. Swift², A. Sydorenko⁸⁶, I. Sykora^{146a}, T. Sykora¹³¹, D. Ta⁸⁶, K. Tackmann⁴⁵,
 J. Taenzer¹⁵⁵, A. Taffard¹⁶⁶, R. Tafirout^{163a}, E. Tahirovic⁷⁹, N. Taiblum¹⁵⁵, H. Takai²⁷, R. Takashima⁷²,
 E.H. Takasugi¹⁰³, K. Takeda⁷⁰, T. Takeshita¹⁴², Y. Takubo⁶⁹, M. Talby⁸⁸, A.A. Talyshev^{111,c}, J. Tanaka¹⁵⁷,
 M. Tanaka¹⁵⁹, R. Tanaka¹¹⁹, R. Tanioka⁷⁰, B.B. Tannenwald¹¹³, S. Tapia Araya^{34b}, S. Tapprogge⁸⁶,
 A. Tarek Abouelfadl Mohamed⁸³, S. Tarem¹⁵⁴, G. Tarna^{28b,p}, G.F. Tartarelli^{94a}, P. Tas¹³¹, M. Tasevsky¹²⁹,
 T. Tashiro⁷¹, E. Tassi^{40a,40b}, A. Tavares Delgado^{128a,128b}, Y. Tayalati^{137e}, A.C. Taylor¹⁰⁷, A.J. Taylor⁴⁹,
 G.N. Taylor⁹¹, P.T.E. Taylor⁹¹, W. Taylor^{163b}, A.S. Tee⁷⁵, P. Teixeira-Dias⁸⁰, D. Temple¹⁴⁴, H. Ten Kate³²,
 P.K. Teng¹⁵³, J.J. Teoh¹²⁰, F. Tepel¹⁷⁷, S. Terada⁶⁹, K. Terashi¹⁵⁷, J. Terron⁸⁵, S. Terzo¹³, M. Testa⁵⁰,
 R.J. Teuscher^{161,n}, S.J. Thais¹⁷⁹, T. Theveneaux-Pelzer⁴⁵, F. Thiele³⁹, J.P. Thomas¹⁹, P.D. Thompson¹⁹,
 A.S. Thompson⁵⁶, L.A. Thomsen¹⁷⁹, E. Thomson¹²⁴, Y. Tian³⁸, R.E. Ticse Torres⁵⁸, V.O. Tikhomirov^{98,ar},
 Yu.A. Tikhonov^{111,c}, S. Timoshenko¹⁰⁰, P. Tipton¹⁷⁹, S. Tisserant⁸⁸, K. Todome¹⁵⁹, S. Todorova-Nova⁵,
 S. Todt⁴⁷, J. Tojo⁷³, S. Tokár^{146a}, K. Tokushuku⁶⁹, E. Tolley¹¹³, M. Tomoto¹⁰⁵, L. Tompkins^{145,as},
 K. Toms¹⁰⁷, B. Tong⁵⁹, P. Tornambe⁵¹, E. Torrence¹¹⁸, H. Torres⁴⁷, E. Torrón Pastor¹⁴⁰, C. Toscirì¹²²,
 J. Toth^{88,at}, F. Touchard⁸⁸, D.R. Tovey¹⁴¹, C.J. Treado¹¹², T. Trefzger¹⁷⁸, F. Tresoldi¹⁵¹, A. Tricoli²⁷,
 I.M. Trigger^{163a}, S. Trincaz-Duvoid⁸³, M.F. Tripiana¹³, W. Trischuk¹⁶¹, B. Trocme⁵⁷, A. Trofymov⁴⁵,
 C. Troncon^{94a}, M. Trovatelli¹⁷², F. Trovato¹⁵¹, L. Truong^{147b}, M. Trzebinski⁴², A. Trzupek⁴², F. Tsai⁴⁵,
 J.C-L. Tseng¹²², P.V. Tsiarehka⁹⁵, N. Tsirintanis⁹, V. Tsiskaridze¹⁵⁰, E.G. Tskhadadze^{54a}, I.I. Tsukerman⁹⁹,
 V. Tsulaia¹⁶, S. Tsuno⁶⁹, D. Tsybychev¹⁵⁰, Y. Tu^{62b}, A. Tudorache^{28b}, V. Tudorache^{28b}, T.T. Tulbure^{28a},
 A.N. Tuna⁵⁹, S. Turchikhin⁶⁸, D. Turgeman¹⁷⁵, I. Turk Cakir^{4b,au}, R. Turra^{94a}, P.M. Tuts³⁸, E. Tzovara⁸⁶,
 G. Ucchielli^{22a,22b}, I. Ueda⁶⁹, M. Ughetto^{148a,148b}, F. Ukegawa¹⁶⁴, G. Unal³², A. Undrus²⁷, G. Unel¹⁶⁶,
 F.C. Ungaro⁹¹, Y. Unno⁶⁹, K. Uno¹⁵⁷, J. Urban^{146b}, P. Urquijo⁹¹, P. Urrejola⁸⁶, G. Usai⁸, J. Usui⁶⁹,
 L. Vacavant⁸⁸, V. Vacek¹³⁰, B. Vachon⁹⁰, K.O.H. Vadla¹²¹, A. Vaidya⁸¹, C. Valderanis¹⁰²,
 E. Valdes Santurio^{148a,148b}, M. Valente⁵², S. Valentinetti^{22a,22b}, A. Valero¹⁷⁰, L. Valéry⁴⁵,
 R.A. Vallance¹⁹, A. Vallier⁵, J.A. Valls Ferrer¹⁷⁰, T.R. Van Daalen¹³, W. Van Den Wollenberg¹⁰⁹,
 H. van der Graaf¹⁰⁹, P. van Gemmeren⁶, J. Van Nieuwkoop¹⁴⁴, I. van Vulpen¹⁰⁹, M.C. van Woerden¹⁰⁹,
 M. Vanadia^{135a,135b}, W. Vandelli³², A. Vaniachine¹⁶⁰, P. Vankov¹⁰⁹, R. Vari^{134a}, E.W. Varnes⁷,
 C. Varni^{53a,53b}, T. Varol⁴³, D. Varouchas¹¹⁹, A. Vartapetian⁸, K.E. Varvell¹⁵², J.G. Vasquez¹⁷⁹,

G.A. Vasquez^{34b}, F. Vazeille³⁷, D. Vazquez Furelos¹³, T. Vazquez Schroeder⁹⁰, J. Veatch⁵⁸, V. Vecchio^{136a,136b}, L.M. Veloce¹⁶¹, F. Veloso^{128a,128c}, S. Veneziano^{134a}, A. Ventura^{76a,76b}, M. Venturi¹⁷², N. Venturi³², V. Vercesi^{123a}, M. Verducci^{136a,136b}, W. Verkerke¹⁰⁹, A.T. Vermeulen¹⁰⁹, J.C. Vermeulen¹⁰⁹, M.C. Vetterli^{144.d}, N. Viaux Maira^{34b}, O. Viazlo⁸⁴, I. Vichou^{169,*}, T. Vickey¹⁴¹, O.E. Vickey Boeriu¹⁴¹, G.H.A. Viehhauser¹²², S. Viel¹⁶, L. Vigani¹²², M. Villa^{22a,22b}, M. Villaplana Perez^{94a,94b}, E. Vilucchi⁵⁰, M.G. Vincter³¹, V.B. Vinogradov⁶⁸, A. Vishwakarma⁴⁵, C. Vittori^{22a,22b}, I. Vivarelli¹⁵¹, S. Vlachos¹⁰, M. Vogel¹⁷⁷, P. Vokac¹³⁰, G. Volpi¹³, S.E. von Buddenbrock^{147c}, E. von Toerne²³, V. Vorobel¹³¹, K. Vorobev¹⁰⁰, M. Vos¹⁷⁰, J.H. Vosseveld⁷⁷, N. Vranjes¹⁴, M. Vranjes Milosavljevic¹⁴, V. Vrba¹³⁰, M. Vreeswijk¹⁰⁹, R. Vuillermet³², I. Vukotic³³, P. Wagner²³, W. Wagner¹⁷⁷, J. Wagner-Kuhr¹⁰², H. Wahlberg⁷⁴, S. Wahrmund⁴⁷, K. Wakamiya⁷⁰, J. Walder⁷⁵, R. Walker¹⁰², W. Walkowiak¹⁴³, V. Wallangen^{148a,148b}, A.M. Wang⁵⁹, C. Wang^{36b,p}, F. Wang¹⁷⁶, H. Wang¹⁶, H. Wang³, J. Wang^{60b}, J. Wang¹⁵², P. Wang⁴³, Q. Wang¹¹⁵, R.-J. Wang⁸³, R. Wang^{36a}, R. Wang⁶, S.M. Wang¹⁵³, W. Wang^{153,av}, W. Wang^{36a,aw}, Y. Wang^{36a}, Z. Wang^{36c}, C. Wanotayaroj⁴⁵, A. Warburton⁹⁰, C.P. Ward³⁰, D.R. Wardrope⁸¹, A. Washbrook⁴⁹, P.M. Watkins¹⁹, A.T. Watson¹⁹, M.F. Watson¹⁹, G. Watts¹⁴⁰, S. Watts⁸⁷, B.M. Waugh⁸¹, A.F. Webb¹¹, S. Webb⁸⁶, C. Weber¹⁷⁹, M.S. Weber¹⁸, S.M. Weber^{60a}, S.A. Weber³¹, J.S. Webster⁶, A.R. Weidberg¹²², B. Weinert⁶⁴, J. Weingarten⁵⁸, M. Weirich⁸⁶, C. Weiser⁵¹, P.S. Wells³², T. Wenaus²⁷, T. Wengler³², S. Wenig³², N. Vermes²³, M.D. Werner⁶⁷, P. Werner³², M. Wessels^{60a}, T.D. Weston¹⁸, K. Whalen¹¹⁸, N.L. Whallon¹⁴⁰, A.M. Wharton⁷⁵, A.S. White⁹², A. White⁸, M.J. White¹, R. White^{34b}, D. Whiteson¹⁶⁶, B.W. Whitmore⁷⁵, F.J. Wickens¹³³, W. Wiedenmann¹⁷⁶, M. Wielers¹³³, C. Wiglesworth³⁹, L.A.M. Wiik-Fuchs⁵¹, A. Wildauer¹⁰³, F. Wilk⁸⁷, H.G. Wilkens³², H.H. Williams¹²⁴, S. Williams³⁰, C. Willis⁹³, S. Willocq⁸⁹, J.A. Wilson¹⁹, I. Wingerter-Seez⁵, E. Winkels¹⁵¹, F. Winklmeier¹¹⁸, O.J. Winston¹⁵¹, B.T. Winter²³, M. Wittgen¹⁴⁵, M. Wobisch^{82.u}, A. Wolf⁸⁶, T.M.H. Wolf¹⁰⁹, R. Wolff⁸⁸, M.W. Wolter⁴², H. Wolters^{128a,128c}, V.W.S. Wong¹⁷¹, N.L. Woods¹³⁹, S.D. Worm¹⁹, B.K. Wosiek⁴², K.W. Wozniak⁴², K. Wraight⁵⁶, M. Wu³³, S.L. Wu¹⁷⁶, X. Wu⁵², Y. Wu^{36a}, T.R. Wyatt⁸⁷, B.M. Wynne⁴⁹, S. Xella³⁹, Z. Xi⁹², L. Xia¹⁷³, D. Xu^{35a}, H. Xu^{36a}, L. Xu²⁷, T. Xu¹³⁸, W. Xu⁹², B. Yabsley¹⁵², S. Yacoob^{147a}, K. Yajima¹²⁰, D.P. Yallup⁸¹, D. Yamaguchi¹⁵⁹, Y. Yamaguchi¹⁵⁹, A. Yamamoto⁶⁹, T. Yamanaka¹⁵⁷, F. Yamane⁷⁰, M. Yamatani¹⁵⁷, T. Yamazaki¹⁵⁷, Y. Yamazaki⁷⁰, Z. Yan²⁴, H. Yang^{36c,36d}, H. Yang¹⁶, S. Yang⁶⁶, Y. Yang¹⁵³, Y. Yang¹⁵⁷, Z. Yang¹⁵, W.-M. Yao¹⁶, Y.C. Yap⁴⁵, Y. Yasu⁶⁹, E. Yatsenko⁵, J. Ye⁴³, S. Ye²⁷, I. Yeletsikh⁶⁸, E. Yigitbasi²⁴, E. Yildirim⁸⁶, K. Yorita¹⁷⁴, K. Yoshihara¹²⁴, C. Young¹⁴⁵, C.J.S. Young³², J. Yu⁸, J. Yu⁶⁷, X. Yue^{60a}, S.P.Y. Yuen²³, I. Yusuff^{30,ax}, B. Zabinski⁴², G. Zacharis¹⁰, E. Zaffaroni⁵², R. Zaidan¹³, A.M. Zaitsev^{132,aj}, N. Zakharchuk⁴⁵, J. Zalieckas¹⁵, S. Zambito⁵⁹, D. Zanzi³², D.R. Zaripovas⁵⁶, C. Zeitnitz¹⁷⁷, G. Zemaityte¹²², J.C. Zeng¹⁶⁹, Q. Zeng¹⁴⁵, O. Zenin¹³², T. Ženiš^{146a}, D. Zerwas¹¹⁹, M. Zgubič¹²², D. Zhang^{36b}, D. Zhang⁹², F. Zhang¹⁷⁶, G. Zhang^{36a,aw}, H. Zhang^{35b}, J. Zhang⁶, L. Zhang⁵¹, L. Zhang^{36a}, M. Zhang¹⁶⁹, P. Zhang^{35b}, R. Zhang²³, R. Zhang^{36a,p}, X. Zhang^{36b}, Y. Zhang^{35a,35d}, Z. Zhang¹¹⁹, X. Zhao⁴³, Y. Zhao^{36b,x}, Z. Zhao^{36a}, A. Zhemchugov⁶⁸, B. Zhou⁹², C. Zhou¹⁷⁶, L. Zhou⁴³, M. Zhou^{35a,35d}, M. Zhou¹⁵⁰, N. Zhou^{36c}, Y. Zhou⁷, C.G. Zhu^{36b}, H. Zhu^{36a}, H. Zhu^{35a}, J. Zhu⁹², Y. Zhu^{36a}, X. Zhuang^{35a}, K. Zhukov⁹⁸, V. Zhulanov^{111,ay}, A. Zibell¹⁷⁸, D. Zieminska⁶⁴, N.I. Zimine⁶⁸, S. Zimmermann⁵¹, Z. Zinonos¹⁰³, M. Zinser⁸⁶, M. Ziolkowski¹⁴³, L. Živković¹⁴, G. Zobernig¹⁷⁶, A. Zoccoli^{22a,22b}, K. Zoch⁵⁸, T.G. Zorbas¹⁴¹, R. Zou³³, M. zur Nedden¹⁷, L. Zwalinski³²

¹ Department of Physics, University of Adelaide, Adelaide, Australia

² Physics Department, SUNY Albany, Albany NY, United States of America

³ Department of Physics, University of Alberta, Edmonton AB, Canada

⁴ (a) Department of Physics, Ankara University, Ankara; (b) Istanbul Aydin University, Istanbul; (c) Division of Physics, TOBB University of Economics and Technology, Ankara, Turkey

⁵ LAPP, Univ. Grenoble Alpes, Univ. Savoie Mont Blanc, CNRS/IN2P3, Annecy, France

⁶ High Energy Physics Division, Argonne National Laboratory, Argonne IL, United States of America

⁷ Department of Physics, University of Arizona, Tucson AZ, United States of America

⁸ Department of Physics, The University of Texas at Arlington, Arlington TX, United States of America

⁹ Physics Department, National and Kapodistrian University of Athens, Athens, Greece

¹⁰ Physics Department, National Technical University of Athens, Zografou, Greece

¹¹ Department of Physics, The University of Texas at Austin, Austin TX, United States of America

¹² Institute of Physics, Azerbaijan Academy of Sciences, Baku, Azerbaijan

¹³ Institut de Física d'Altes Energies (IFAE), The Barcelona Institute of Science and Technology, Barcelona, Spain

¹⁴ Institute of Physics, University of Belgrade, Belgrade, Serbia

¹⁵ Department for Physics and Technology, University of Bergen, Bergen, Norway

¹⁶ Physics Division, Lawrence Berkeley National Laboratory and University of California, Berkeley CA, United States of America

- ¹⁷ Department of Physics, Humboldt University, Berlin, Germany
- ¹⁸ Albert Einstein Center for Fundamental Physics and Laboratory for High Energy Physics, University of Bern, Bern, Switzerland
- ¹⁹ School of Physics and Astronomy, University of Birmingham, Birmingham, United Kingdom
- ²⁰ ^(a) Department of Physics, Bogazici University, Istanbul; ^(b) Department of Physics Engineering, Gaziantep University, Gaziantep; ^(d) Istanbul Bilgi University, Faculty of Engineering and Natural Sciences, Istanbul; ^(e) Bahcesehir University, Faculty of Engineering and Natural Sciences, Istanbul, Turkey
- ²¹ Centro de Investigaciones, Universidad Antonio Narino, Bogota, Colombia
- ²² ^(a) INFN Sezione di Bologna; ^(b) Dipartimento di Fisica e Astronomia, Università di Bologna, Bologna, Italy
- ²³ Physikalisches Institut, University of Bonn, Bonn, Germany
- ²⁴ Department of Physics, Boston University, Boston MA, United States of America
- ²⁵ Department of Physics, Brandeis University, Waltham MA, United States of America
- ²⁶ ^(a) Universidade Federal do Rio De Janeiro COPPE/EE/IF, Rio de Janeiro; ^(b) Electrical Circuits Department, Federal University of Juiz de Fora (UFJF), Juiz de Fora; ^(c) Federal University of Sao Joao del Rei (UFSJ), Sao Joao del Rei; ^(d) Instituto de Fisica, Universidade de Sao Paulo, Sao Paulo, Brazil
- ²⁷ Physics Department, Brookhaven National Laboratory, Upton NY, United States of America
- ²⁸ ^(a) Transilvania University of Brasov, Brasov; ^(b) Horia Hulubei National Institute of Physics and Nuclear Engineering, Bucharest; ^(c) Department of Physics, Alexandru Ioan Cuza University of Iasi, Iasi; ^(d) National Institute for Research and Development of Isotopic and Molecular Technologies, Physics Department, Cluj Napoca; ^(e) University Politehnica Bucharest, Bucharest; ^(f) West University in Timisoara, Timisoara, Romania
- ²⁹ Departamento de Física, Universidad de Buenos Aires, Buenos Aires, Argentina
- ³⁰ Cavendish Laboratory, University of Cambridge, Cambridge, United Kingdom
- ³¹ Department of Physics, Carleton University, Ottawa ON, Canada
- ³² CERN, Geneva, Switzerland
- ³³ Enrico Fermi Institute, University of Chicago, Chicago IL, United States of America
- ³⁴ ^(a) Departamento de Física, Pontificia Universidad Católica de Chile, Santiago; ^(b) Departamento de Física, Universidad Técnica Federico Santa María, Valparaíso, Chile
- ³⁵ ^(a) Institute of High Energy Physics, Chinese Academy of Sciences, Beijing; ^(b) Department of Physics, Nanjing University, Jiangsu; ^(c) Physics Department, Tsinghua University, Beijing 100084; ^(d) University of Chinese Academy of Science (UCAS), Beijing, China
- ³⁶ ^(a) Department of Modern Physics and State Key Laboratory of Particle Detection and Electronics, University of Science and Technology of China, Anhui; ^(b) School of Physics, Shandong University, Shandong; ^(c) School of Physics and Astronomy, Key Laboratory for Particle Physics, Astrophysics and Cosmology, Ministry of Education; Shanghai Key Laboratory for Particle Physics and Cosmology, Shanghai Jiao Tong University; ^(d) Tsung-Dao Lee Institute, Shanghai, China
- ³⁷ Université Clermont Auvergne, CNRS/IN2P3, LPC, Clermont-Ferrand, France
- ³⁸ Nevis Laboratory, Columbia University, Irvington NY, United States of America
- ³⁹ Niels Bohr Institute, University of Copenhagen, Kobenhavn, Denmark
- ⁴⁰ ^(a) INFN Gruppo Collegato di Cosenza, Laboratori Nazionali di Frascati; ^(b) Dipartimento di Fisica, Università della Calabria, Rende, Italy
- ⁴¹ ^(a) AGH University of Science and Technology, Faculty of Physics and Applied Computer Science, Krakow; ^(b) Marian Smoluchowski Institute of Physics, Jagiellonian University, Krakow, Poland
- ⁴² Institute of Nuclear Physics Polish Academy of Sciences, Krakow, Poland
- ⁴³ Physics Department, Southern Methodist University, Dallas TX, United States of America
- ⁴⁴ Physics Department, University of Texas at Dallas, Richardson TX, United States of America
- ⁴⁵ DESY, Hamburg and Zeuthen, Germany
- ⁴⁶ Lehrstuhl für Experimentelle Physik IV, Technische Universität Dortmund, Dortmund, Germany
- ⁴⁷ Institut für Kern- und Teilchenphysik, Technische Universität Dresden, Dresden, Germany
- ⁴⁸ Department of Physics, Duke University, Durham NC, United States of America
- ⁴⁹ SUPA – School of Physics and Astronomy, University of Edinburgh, Edinburgh, United Kingdom
- ⁵⁰ INFN e Laboratori Nazionali di Frascati, Frascati, Italy
- ⁵¹ Fakultät für Mathematik und Physik, Albert-Ludwigs-Universität, Freiburg, Germany
- ⁵² Departement de Physique Nucleaire et Corpusculaire, Université de Genève, Geneva, Switzerland
- ⁵³ ^(a) INFN Sezione di Genova; ^(b) Dipartimento di Fisica, Università di Genova, Genova, Italy
- ⁵⁴ ^(a) E. Andronikashvili Institute of Physics, Iv. Javakishvili Tbilisi State University, Tbilisi; ^(b) High Energy Physics Institute, Tbilisi State University, Tbilisi, Georgia
- ⁵⁵ II. Physikalisches Institut, Justus-Liebig-Universität Giessen, Giessen, Germany
- ⁵⁶ SUPA – School of Physics and Astronomy, University of Glasgow, Glasgow, United Kingdom
- ⁵⁷ LPSC, Université Grenoble Alpes, CNRS-IN2P3, Grenoble INP, Grenoble, France
- ⁵⁸ II Physikalisches Institut, Georg-August-Universität, Göttingen, Germany
- ⁵⁹ Laboratory for Particle Physics and Cosmology, Harvard University, Cambridge MA, United States of America
- ⁶⁰ ^(a) Kirchhoff-Institut für Physik, Ruprecht-Karls-Universität Heidelberg, Heidelberg; ^(b) Physikalisches Institut, Ruprecht-Karls-Universität Heidelberg, Heidelberg, Germany
- ⁶¹ Faculty of Applied Information Science, Hiroshima Institute of Technology, Hiroshima, Japan
- ⁶² ^(a) Department of Physics, The Chinese University of Hong Kong, Shatin, N.T., Hong Kong; ^(b) Department of Physics, The University of Hong Kong, Hong Kong; ^(c) Department of Physics and Institute for Advanced Study, The Hong Kong University of Science and Technology, Clear Water Bay, Kowloon, Hong Kong, China
- ⁶³ Department of Physics, National Tsing Hua University, Hsinchu, Taiwan
- ⁶⁴ Department of Physics, Indiana University, Bloomington IN, United States of America
- ⁶⁵ Institut für Astro- und Teilchenphysik, Leopold-Franzens-Universität, Innsbruck, Austria
- ⁶⁶ University of Iowa, Iowa City IA, United States of America
- ⁶⁷ Department of Physics and Astronomy, Iowa State University, Ames IA, United States of America
- ⁶⁸ Joint Institute for Nuclear Research, JINR Dubna, Dubna, Russia
- ⁶⁹ KEK, High Energy Accelerator Research Organization, Tsukuba, Japan
- ⁷⁰ Graduate School of Science, Kobe University, Kobe, Japan
- ⁷¹ Faculty of Science, Kyoto University, Kyoto, Japan
- ⁷² Kyoto University of Education, Kyoto, Japan
- ⁷³ Research Center for Advanced Particle Physics and Department of Physics, Kyushu University, Fukuoka, Japan
- ⁷⁴ Instituto de Física La Plata, Universidad Nacional de La Plata and CONICET, La Plata, Argentina
- ⁷⁵ Physics Department, Lancaster University, Lancaster, United Kingdom
- ⁷⁶ ^(a) INFN Sezione di Lecce; ^(b) Dipartimento di Matematica e Fisica, Università del Salento, Lecce, Italy
- ⁷⁷ Oliver Lodge Laboratory, University of Liverpool, Liverpool, United Kingdom
- ⁷⁸ Department of Experimental Particle Physics, Jožef Stefan Institute and Department of Physics, University of Ljubljana, Ljubljana, Slovenia
- ⁷⁹ School of Physics and Astronomy, Queen Mary University of London, London, United Kingdom
- ⁸⁰ Department of Physics, Royal Holloway University of London, Surrey, United Kingdom
- ⁸¹ Department of Physics and Astronomy, University College London, London, United Kingdom
- ⁸² Louisiana Tech University, Ruston LA, United States of America
- ⁸³ Laboratoire de Physique Nucléaire et de Hautes Energies, UPMC and Université Paris-Diderot and CNRS/IN2P3, Paris, France
- ⁸⁴ Fysiska institutionen, Lunds universitet, Lund, Sweden
- ⁸⁵ Departamento de Física Teórica C-15 and CIAFF, Universidad Autónoma de Madrid, Madrid, Spain
- ⁸⁶ Institut für Physik, Universität Mainz, Mainz, Germany

- ⁸⁷ School of Physics and Astronomy, University of Manchester, Manchester, United Kingdom
- ⁸⁸ CPPM, Aix-Marseille Université and CNRS/IN2P3, Marseille, France
- ⁸⁹ Department of Physics, University of Massachusetts, Amherst MA, United States of America
- ⁹⁰ Department of Physics, McGill University, Montreal QC, Canada
- ⁹¹ School of Physics, University of Melbourne, Victoria, Australia
- ⁹² Department of Physics, The University of Michigan, Ann Arbor MI, United States of America
- ⁹³ Department of Physics and Astronomy, Michigan State University, East Lansing MI, United States of America
- ⁹⁴ ^(a) INFN Sezione di Milano; ^(b) Dipartimento di Fisica, Università di Milano, Milano, Italy
- ⁹⁵ B.I. Stepanov Institute of Physics, National Academy of Sciences of Belarus, Minsk, Belarus
- ⁹⁶ Research Institute for Nuclear Problems of Byelorussian State University, Minsk, Belarus
- ⁹⁷ Group of Particle Physics, University of Montreal, Montreal QC, Canada
- ⁹⁸ P.N. Lebedev Physical Institute of the Russian Academy of Sciences, Moscow, Russia
- ⁹⁹ Institute for Theoretical and Experimental Physics (ITEP), Moscow, Russia
- ¹⁰⁰ National Research Nuclear University MEPhI, Moscow, Russia
- ¹⁰¹ D.V. Skobeltsyn Institute of Nuclear Physics, M.V. Lomonosov Moscow State University, Moscow, Russia
- ¹⁰² Fakultät für Physik, Ludwig-Maximilians-Universität München, München, Germany
- ¹⁰³ Max-Planck-Institut für Physik (Werner-Heisenberg-Institut), München, Germany
- ¹⁰⁴ Nagasaki Institute of Applied Science, Nagasaki, Japan
- ¹⁰⁵ Graduate School of Science and Kobayashi–Maskawa Institute, Nagoya University, Nagoya, Japan
- ¹⁰⁶ ^(a) INFN Sezione di Napoli; ^(b) Dipartimento di Fisica, Università di Napoli, Napoli, Italy
- ¹⁰⁷ Department of Physics and Astronomy, University of New Mexico, Albuquerque NM, United States of America
- ¹⁰⁸ Institute for Mathematics, Astrophysics and Particle Physics, Radboud University Nijmegen/Nikhef, Nijmegen, Netherlands
- ¹⁰⁹ Nikhef National Institute for Subatomic Physics and University of Amsterdam, Amsterdam, Netherlands
- ¹¹⁰ Department of Physics, Northern Illinois University, DeKalb IL, United States of America
- ¹¹¹ Budker Institute of Nuclear Physics, SB RAS, Novosibirsk, Russia
- ¹¹² Department of Physics, New York University, New York NY, United States of America
- ¹¹³ Ohio State University, Columbus OH, United States of America
- ¹¹⁴ Faculty of Science, Okayama University, Okayama, Japan
- ¹¹⁵ Homer L. Dodge Department of Physics and Astronomy, University of Oklahoma, Norman OK, United States of America
- ¹¹⁶ Department of Physics, Oklahoma State University, Stillwater OK, United States of America
- ¹¹⁷ Palacký University, RCPTM, Olomouc, Czech Republic
- ¹¹⁸ Center for High Energy Physics, University of Oregon, Eugene OR, United States of America
- ¹¹⁹ LAL, Univ. Paris-Sud, CNRS/IN2P3, Université Paris-Saclay, Orsay, France
- ¹²⁰ Graduate School of Science, Osaka University, Osaka, Japan
- ¹²¹ Department of Physics, University of Oslo, Oslo, Norway
- ¹²² Department of Physics, Oxford University, Oxford, United Kingdom
- ¹²³ ^(a) INFN Sezione di Pavia; ^(b) Dipartimento di Fisica, Università di Pavia, Pavia, Italy
- ¹²⁴ Department of Physics, University of Pennsylvania, Philadelphia PA, United States of America
- ¹²⁵ National Research Centre “Kurchatov Institute” B.P. Konstantinov Petersburg Nuclear Physics Institute, St. Petersburg, Russia
- ¹²⁶ ^(a) INFN Sezione di Pisa; ^(b) Dipartimento di Fisica E. Fermi, Università di Pisa, Pisa, Italy
- ¹²⁷ Department of Physics and Astronomy, University of Pittsburgh, Pittsburgh PA, United States of America
- ¹²⁸ ^(a) Laboratório de Instrumentação e Física Experimental de Partículas – LIP, Lisboa; ^(b) Faculdade de Ciências, Universidade de Lisboa, Lisboa; ^(c) Department of Physics, University of Coimbra, Coimbra; ^(e) Departamento de Física, Universidade do Minho, Braga; ^(f) Departamento de Física Teórica y del Cosmos, Universidad de Granada, Granada, Spain; ^(g) Dep Física and CEFITEC de Faculdade de Ciências e Tecnologia, Universidade Nova de Lisboa, Caparica, Portugal
- ¹²⁹ Institute of Physics, Academy of Sciences of the Czech Republic, Praha, Czech Republic
- ¹³⁰ Czech Technical University in Prague, Praha, Czech Republic
- ¹³¹ Charles University, Faculty of Mathematics and Physics, Prague, Czech Republic
- ¹³² State Research Center Institute for High Energy Physics (Protvino), NRC KI, Russia
- ¹³³ Particle Physics Department, Rutherford Appleton Laboratory, Didcot, United Kingdom
- ¹³⁴ ^(a) INFN Sezione di Roma; ^(b) Dipartimento di Fisica, Sapienza Università di Roma, Roma, Italy
- ¹³⁵ ^(a) INFN Sezione di Roma Tor Vergata; ^(b) Dipartimento di Fisica, Università di Roma Tor Vergata, Roma, Italy
- ¹³⁶ ^(a) INFN Sezione di Roma Tre; ^(b) Dipartimento di Matematica e Fisica, Università Roma Tre, Roma, Italy
- ¹³⁷ ^(a) Faculté des Sciences Ain Chock, Réseau Universitaire de Physique des Hautes Energies – Université Hassan II, Casablanca; ^(b) Centre National de l’Energie des Sciences Techniques Nucleaires, Rabat; ^(c) Faculté des Sciences Semlalia, Université Cadi Ayyad, LPHEA-Marrakech; ^(d) Faculté des Sciences, Université Mohamed Premier and LPTPM, Oujda; ^(e) Faculté des sciences, Université Mohammed V, Rabat, Morocco
- ¹³⁸ Institut de Recherches sur les Lois Fondamentales de l’Univers, DSM/IRFU, CEA Saclay, Gif-sur-Yvette, France
- ¹³⁹ Santa Cruz Institute for Particle Physics, University of California Santa Cruz, Santa Cruz CA, United States of America
- ¹⁴⁰ Department of Physics, University of Washington, Seattle WA, United States of America
- ¹⁴¹ Department of Physics and Astronomy, University of Sheffield, Sheffield, United Kingdom
- ¹⁴² Department of Physics, Shinshu University, Nagano, Japan
- ¹⁴³ Department Physik, Universität Siegen, Siegen, Germany
- ¹⁴⁴ Department of Physics, Simon Fraser University, Burnaby BC, Canada
- ¹⁴⁵ SLAC National Accelerator Laboratory, Stanford CA, United States of America
- ¹⁴⁶ ^(a) Faculty of Mathematics, Physics & Informatics, Comenius University, Bratislava; ^(b) Department of Subnuclear Physics, Institute of Experimental Physics of the Slovak Academy of Sciences, Kosice, Slovak Republic
- ¹⁴⁷ ^(a) Department of Physics, University of Cape Town, Cape Town; ^(b) Department of Mechanical Engineering Science, University of Johannesburg, Johannesburg; ^(c) School of Physics, University of the Witwatersrand, Johannesburg, South Africa
- ¹⁴⁸ ^(a) Department of Physics, Stockholm University; ^(b) The Oskar Klein Centre, Stockholm, Sweden
- ¹⁴⁹ Physics Department, Royal Institute of Technology, Stockholm, Sweden
- ¹⁵⁰ Departments of Physics & Astronomy and Chemistry, Stony Brook University, Stony Brook NY, United States of America
- ¹⁵¹ Department of Physics and Astronomy, University of Sussex, Brighton, United Kingdom
- ¹⁵² School of Physics, University of Sydney, Sydney, Australia
- ¹⁵³ Institute of Physics, Academia Sinica, Taipei, Taiwan
- ¹⁵⁴ Department of Physics, Technion: Israel Institute of Technology, Haifa, Israel
- ¹⁵⁵ Raymond and Beverly Sackler School of Physics and Astronomy, Tel Aviv University, Tel Aviv, Israel
- ¹⁵⁶ Department of Physics, Aristotle University of Thessaloniki, Thessaloniki, Greece
- ¹⁵⁷ International Center for Elementary Particle Physics and Department of Physics, The University of Tokyo, Tokyo, Japan
- ¹⁵⁸ Graduate School of Science and Technology, Tokyo Metropolitan University, Tokyo, Japan
- ¹⁵⁹ Department of Physics, Tokyo Institute of Technology, Tokyo, Japan

- ¹⁶⁰ Tomsk State University, Tomsk, Russia
¹⁶¹ Department of Physics, University of Toronto, Toronto ON, Canada
¹⁶² ^(a) INFN-TIFPA; ^(b) University of Trento, Trento, Italy
¹⁶³ ^(a) TRIUMF, Vancouver BC; ^(b) Department of Physics and Astronomy, York University, Toronto ON, Canada
¹⁶⁴ Division of Physics and Tomonaga Center for the History of the Universe, Faculty of Pure and Applied Sciences, University of Tsukuba, Tsukuba, Japan
¹⁶⁵ Department of Physics and Astronomy, Tufts University, Medford MA, United States of America
¹⁶⁶ Department of Physics and Astronomy, University of California Irvine, Irvine CA, United States of America
¹⁶⁷ ^(a) INFN Gruppo Collegato di Udine, Sezione di Trieste, Udine; ^(b) ICTP, Trieste; ^(c) Dipartimento di Chimica, Fisica e Ambiente, Università di Udine, Udine, Italy
¹⁶⁸ Department of Physics and Astronomy, University of Uppsala, Uppsala, Sweden
¹⁶⁹ Department of Physics, University of Illinois, Urbana IL, United States of America
¹⁷⁰ Instituto de Física Corpuscular (IFIC), Centro Mixto Universidad de Valencia – CSIC, Spain
¹⁷¹ Department of Physics, University of British Columbia, Vancouver BC, Canada
¹⁷² Department of Physics and Astronomy, University of Victoria, Victoria BC, Canada
¹⁷³ Department of Physics, University of Warwick, Coventry, United Kingdom
¹⁷⁴ Waseda University, Tokyo, Japan
¹⁷⁵ Department of Particle Physics, The Weizmann Institute of Science, Rehovot, Israel
¹⁷⁶ Department of Physics, University of Wisconsin, Madison WI, United States of America
¹⁷⁷ Fakultät für Mathematik und Naturwissenschaften, Fachgruppe Physik, Bergische Universität Wuppertal, Wuppertal, Germany
¹⁷⁸ Fakultät für Physik und Astronomie, Julius-Maximilians-Universität, Würzburg, Germany
¹⁷⁹ Department of Physics, Yale University, New Haven CT, United States of America
¹⁸⁰ Yerevan Physics Institute, Yerevan, Armenia
¹⁸¹ Centre de Calcul de l'Institut National de Physique Nucléaire et de Physique des Particules (IN2P3), Villeurbanne, France
¹⁸² Academia Sinica Grid Computing, Institute of Physics, Academia Sinica, Taipei, Taiwan

^a Also at Department of Physics, King's College London, London, United Kingdom.

^b Also at Institute of Physics, Azerbaijan Academy of Sciences, Baku, Azerbaijan.

^c Also at Novosibirsk State University, Novosibirsk, Russia.

^d Also at TRIUMF, Vancouver BC, Canada.

^e Also at Department of Physics & Astronomy, University of Louisville, Louisville, KY, United States of America.

^f Also at Physics Department, An-Najah National University, Nablus, Palestine.

^g Also at Department of Physics, California State University, Fresno CA, United States of America.

^h Also at Department of Physics, University of Fribourg, Fribourg, Switzerland.

ⁱ Also at II Physikalisches Institut, Georg-August-Universität, Göttingen, Germany.

^j Also at Departament de Física de la Universitat Autònoma de Barcelona, Barcelona, Spain.

^k Also at Tomsk State University, Tomsk, and Moscow Institute of Physics and Technology State University, Dolgoprudny, Russia.

^l Also at The Collaborative Innovation Center of Quantum Matter (CICQM), Beijing, China.

^m Also at Università di Napoli Parthenope, Napoli, Italy.

ⁿ Also at Institute of Particle Physics (IPP), Canada.

^o Also at Horia Hulubei National Institute of Physics and Nuclear Engineering, Bucharest, Romania.

^p Also at CPPM, Aix-Marseille Université and CNRS/IN2P3, Marseille, France.

^q Also at Department of Physics, St. Petersburg State Polytechnical University, St. Petersburg, Russia.

^r Also at Borough of Manhattan Community College, City University of New York, New York City, United States of America.

^s Also at Department of Financial and Management Engineering, University of the Aegean, Chios, Greece.

^t Also at Centre for High Performance Computing, CSIR Campus, Rosebank, Cape Town, South Africa.

^u Also at Louisiana Tech University, Ruston LA, United States of America.

^v Also at Institutio Catalana de Recerca i Estudis Avançats, ICREA, Barcelona, Spain.

^w Also at Department of Physics, The University of Michigan, Ann Arbor MI, United States of America.

^x Also at LAL, Univ. Paris-Sud, CNRS/IN2P3, Université Paris-Saclay, Orsay, France.

^y Also at Graduate School of Science, Osaka University, Osaka, Japan.

^z Also at Fakultät für Mathematik und Physik, Albert-Ludwigs-Universität, Freiburg, Germany.

^{aa} Also at Institute for Mathematics, Astrophysics and Particle Physics, Radboud University Nijmegen/Nikhef, Nijmegen, Netherlands.

^{ab} Also at Institute of Theoretical Physics, Ilia State University, Tbilisi, Georgia.

^{ac} Also at CERN, Geneva, Switzerland.

^{ad} Also at Georgian Technical University (GTU), Tbilisi, Georgia.

^{ae} Also at Manhattan College, New York NY, United States of America.

^{af} Also at Hellenic Open University, Patras, Greece.

^{ag} Also at The City College of New York, New York NY, United States of America.

^{ah} Also at Departamento de Física Teórica y del Cosmos, Universidad de Granada, Granada, Portugal.

^{ai} Also at Department of Physics, California State University, Sacramento CA, United States of America.

^{aj} Also at Moscow Institute of Physics and Technology State University, Dolgoprudny, Russia.

^{ak} Also at Ochadai Academic Production, Ochanomizu University, Tokyo, Japan.

^{al} Also at Departement de Physique Nucleaire et Corpusculaire, Université de Genève, Geneva, Switzerland.

^{am} Also at Department of Physics, The University of Texas at Austin, Austin TX, United States of America.

^{an} Also at Institut de Física d'Altes Energies (IFAE), The Barcelona Institute of Science and Technology, Barcelona, Spain.

^{ao} Also at School of Physics, Sun Yat-sen University, Guangzhou, China.

^{ap} Also at Institute for Nuclear Research and Nuclear Energy (INRNE) of the Bulgarian Academy of Sciences, Sofia, Bulgaria.

^{aq} Also at Faculty of Physics, M.V. Lomonosov Moscow State University, Moscow, Russia.

^{ar} Also at National Research Nuclear University MEPhI, Moscow, Russia.

^{as} Also at Department of Physics, Stanford University, Stanford CA, United States of America.

^{at} Also at Institute for Particle and Nuclear Physics, Wigner Research Centre for Physics, Budapest, Hungary.

^{au} Also at Giresun University, Faculty of Engineering, Turkey.

^{av} Also at Department of Physics, Nanjing University, Jiangsu, China.

^{aw} Also at Institute of Physics, Academia Sinica, Taipei, Taiwan.

^{ax} Also at University of Malaya, Department of Physics, Kuala Lumpur, Malaysia.

^{ay} Also at Budker Institute of Nuclear Physics, SB RAS, Novosibirsk, Russia.

^{az} Also at Dipartimento di Fisica E. Fermi, Università di Pisa, Pisa, Italy.

^{ba} Also at Near East University, Nicosia, North Cyprus, Mersin 10, Turkey.

^{bb} Also at Faculdade de Ciências, Universidade de Lisboa, Lisboa, Portugal.

* Deceased.